

LINTING OF FILLER IN THE OFFSET PRINTING PROCESS

This Minor Thesis is submitted as a requirement for the degree of Masters of Engineering Science in Pulp and Paper Technology at the Australian Pulp and Paper Institute, Department of Chemical Engineering, Monash University, Clayton, Victoria, Australia

April 2004

SONYA F. RAND
B.E. (Chemical), University of Adelaide

Australian Pulp and Paper Institute
Monash University

CONTENTS

	Page
SUMMARY	4
DECLARATION	7
ACKNOWLEDGEMENTS	8
1.0 INTRODUCTION	9
2.0 LITERATURE REVIEW	13
3.0 EXPERIMENTAL	29
3.1 Printing Experiments	29
3.1.1 IGT Testing	29
3.1.2 Quantification of Lint Removed	33
3.1.2.1 <i>Image Analysis of Printed Paper</i>	33
3.1.2.2 <i>Image Analysis of Lint</i>	36
3.1.3 Heidelberg Print Tests	40
3.2 Filler Size Distribution	41
3.2.1 SEM / Backscatter	42
3.2.1.1 <i>Sample Preparation</i>	42
3.2.1.2 <i>Microscopic Analysis</i>	42
3.2.1.3 <i>Image Analysis</i>	51
3.2.2 SE Microprobe with X-Ray Detection	56
3.2.2.1 <i>Sample Preparation</i>	57
3.2.2.2 <i>Microscopic Analysis</i>	59
3.2.3 X-Ray Tomography with Phase Contrast	62
3.2.4 FTIR Spectroscopy	70
3.2.4.1 <i>Determination of spectra</i>	70
3.2.4.2 <i>Paper measurement</i>	74

4.0 RESULTS AND DISCUSSION	77
5.0 CONCLUSIONS	85
6.0 RECOMMENDATIONS FOR FURTHER WORK	87
7.0 REFERENCES	89
APPENDIX A - Norske Skog Procedure for IGT Testing	92
APPENDIX B - National Print Laboratory, Procedure for IGT Testing	98
APPENDIX C – Experimental Matrix for IGT Experiments	101
APPENDIX D – Ink Weight on Printed IGT samples	103
APPENDIX E – Quantification of Printed IGT Lint	104
APPENDIX F – Heidelberg Lint Test – Test Pattern	105
APPENDIX G – Particle Size Distribution of Filler in SEM backscatter images	106
APPENDIX H – Specification sheet for Image / Norstar 52 gsm	108
APPENDIX I – Heidelberg Test results	109

SUMMARY

The aim of this project is to predict the filler linting propensity of newsprint by the following process :

- a. Design printing experiments to artificially remove filler from the surface of machine made newsprint
- b. Investigate novel methods of determining filler size distribution in paper
- c. Compare the material removed in the laboratory printing experiments with the filler size distributions measured in the surface of the paper

Norske Skog Boyer Mill supplied samples of newsprint for analysis. These were chosen as they had a known propensity to lint, from quality and audit testing conducted at the paper mill. The quality testing included running 7,000 sheets through a small sheet fed offset press and measuring the mass of material removed.

Printing experiments were designed to artificially remove filler from the surface of the newsprint using an IGT Printability Tester. This test was able to demonstrate the linting propensity of a series of newsprint samples.

Image Analysis was used to quantify the lint removed from the newsprint in the printing experiments.

Several methods of determining filler size distribution in paper were investigated including:

- a. Scanning electron Microscopy (SEM) with backscatter detection
- b. Scanning electron Microscopy (SEM) with x-ray detection
- c. Scanning electron Microprobe with x-ray detection
- d. X-Ray Tomography with Phase contrast
- e. FTIR Spectroscopy

Scanning electron Microscopy (SEM) with backscatter detection was the most successful method for determining the size distribution of filler particles in the newsprint surface.

No correlation could be found between the material removed in the laboratory printing experiments and the filler size distributions measured in the surface of the paper.

Correlations were found between the Treeline result in the offset printing test run by Norske Skog, and the degree of linting of the IGT test print.

Correlations were found between the Treeline result, and the amount of filler measured in the surface of the sheet by SEM and backscatter detection.

Recommendations for future work include the following:

- a. Investigate the ability of FTIR Spectroscopy quantify filler size distribution on newsprint surfaces.
- b. Repeat the IGT experimental set, including the addition of water / fountain solution as a variable.
- c. Obtain more data for treeline results to confirm correlations obtained.

DECLARATION

I, Sonya Rand hereby declare that this minor thesis contains no material which has been accepted for the award of any other degree or diploma in any university and that, to the best of my knowledge and belief, contains no material previously published or written by another person, except where due reference is made.

Signed.....

Date.....

ACKNOWLEDGEMENTS

The author would like to acknowledge the following companies and individuals for their assistance and support in undertaking this minor thesis:

- My thesis supervisor at APPI, Warren Batchelor
- Dianne Richards at APPI
- Rodolphe Koehly at APPI
- Pavel Janko at APPI
- Mark Greaves and John Ward at CSIRO, Division of Forestry and Forest Products
- Dave Watkins and John McConnell at the National Print Laboratory
- Paul Banham, Tony Flowers and Philip Dingle at Norske Skog, Australian and New Zealand Mills
- Julie Sheffield-Parker at XRT Limited
- Sel Glanville at Monash University, School of Physics and Materials Engineering
- Finlay Shanks at Monash University, Department of Chemistry
- Gregory Suzor, my husband

1.0 INTRODUCTION

In the offset printing of newsprint, linting is described as the tendency of paper to shed loosely bound fibres and fines during printing.[1] This material subsequently adheres to the offset printing blanket and disrupts the transfer of ink from the inking system to the blanket. The result is a deterioration of print quality to the point where the press must be stopped and cleaned.[2]

The international industry trend has been an increase in offset printing of newsprint and hence linting is a major source of customer complaints to paper manufacturers.[2-5] All newspapers in Australia are printed using the offset process.

The mechanism of linting is generally described as a combined effect on the ink film splitting forces and the inter fibre bonding energy of the paper surface.[2],[4] Linting is also related to the flow of ink in the press nip under pressure. There are two types of ink flows : a porous ink flow, penetrating the paper surface pores and a free ink flow at the surface of the ink-saturated pores. Theoretical analysis by Mangin and Silvy [6] shows that the ink flows induce sufficient drag on the fibre to cause lint by disturbing the bonding of weakly bound fibres on the surface.

Researchers [2],[7] suggest that different levels of force applied to the surface of paper generate different types of linting. At low forces, unbonded material, often referred to as dust, is removed. At medium forces, weak or loosely bound material, often referred to as lint is removed. At higher forces, well bonded surface fibres are removed, often referred to as picking.

The lint removed from an offset blanket ranges in size from very fine fibre and filler fragments, ray cells, whole fibres to mini shives and other debris.[4],[8-9] Ray cells are the predominant component of lint, followed by fibre fragments, poorly fibrillated fibres and fillers.[2]

Whilst paper manufacturers are investing substantial effort into understanding and preventing linting of papers, it is not only due to paper issues. Linting arises from a complex interaction between paper properties and printing press parameters.

Some studies have suggested that the printing press variables have a greater effect on the linting propensity of paper than the paper itself.[2]

Norske Skog, manufacturers of newsprint have initiated a technical study of linting in relation to offset printing of newsprint. This study is a collaborative effort between Norske Skog paper mills in Europe, Australia and New Zealand and external research providers.

The work reported in this thesis is part of the collaborative work between the CRC for Functional Communication Surfaces, Australian Pulp and Paper Institute and Norske Skog. The work reported is part of a broader linting project. Other researchers in the project are studying the linting of fibre.

The aim of this project is to predict the filler linting propensity of newsprint by the following process :

1. Design printing experiments to artificially remove filler from the surface of machine made newsprint
2. Investigate novel methods of determining filler size distribution in paper
3. Compare the material removed in the laboratory printing experiments with the filler size distributions measured in the surface of the paper

Paper from Norske Skog, Boyer Mill, Tasmania forms the basis for this study. Norske Skog Boyer Mill, employs 450 people and manufactures a range of newsprint and publishing related grades. The 290,000 tonnes of paper produced represents 40 % of the Australian market

Raw materials for the mill are plantation radiata pine, regrowth eucalypt and recycled fibre, which is produced at Norske Skog, Albury Mill, NSW.

There are 2 paper machines on site, PM2 and PM3 with production capacities of 125 000 tpa and 165 000 tpa respectively.

The paper grade used for the study is named Image / Norstar and is a 52 gsm improved newsprint grade manufactured on PM2. The specifications for Image / Norstar are given in Appendix H. The furnish is 67 % TMP radiata pine, 28 % chemi-mechanical eucalypt (cold caustic soda) and a filler component of 5 % calcined clay (supplied by Imerys as Alphatex).

This paper grade was chosen for analysis as it has been subject to linting in the past, according to customer feedback and in house quality and audit checks.

It is anticipated that further research in the topic of linting, will provide a more detailed understanding of the mechanism and assist in determining ways to minimise its occurrence.

2.0 LITERATURE REVIEW

This literature review addresses the linting of fibre and fillers from newsprint and offset printed papers. The published literature pertaining to linting focuses on fibre linting as it is perceived to be greater in impact and magnitude. Generally, where fibre linting occurs, filler will also be present in the lint removed. There is a general lack of research and literature on the specific linting of filler from newsprint and hence this body of work is aimed at improving the understanding of this phenomena.

Filler is added to the sheet for a variety of reasons : [10]

- Increase of brightness and opacity
- Improve sheet formation
- Improve print characteristics
- Replacement of expensive fibre material.

These aims can only be achieved if the filler is retained in the sheet with a uniform filler distribution. It is when filler separates from the sheet structure that linting and dusting problems start to occur. [10]

Retention aids are added in the papermaking process to improve filler retention in the sheet. Typically, cationic synthetic polymers, two component soluble polymer systems or micro-particulate systems are used to achieve the filler retention. [11] The measurement of filler retention on the paper machine does not however necessarily take into account the filler distribution throughout the sheet.

All retention aid systems based on high molecular weight polymers such as polyacrylamides have a tendency to flocculate the filler particles into large aggregates, but do not provide a uniform filler distribution throughout the sheet. [11]

Studies have been conducted [10],[11] that suggest that filler linting propensity increases where there is a high degree of agglomeration of the filler as opposed to a uniform filler distribution in the sheet.

Alternative methods such as treating the filler with high charge density low molecular weight polyethylene enables the filler to link as small particles to the fibre structure. [11]

The propensity of filler to lint out of the sheet is also based on its location in the thickness of the sheet. Filler particles on the surface of the sheet are more likely to be lint candidates. The distribution of filler in the thickness of the sheet is a function of the forming and dewatering conditions on the paper machine. Vacuum and forming conditions should be optimized to ensure that the filler distribution is even and not localised on the sheet surface. For these reasons, paper made in a gap former is less likely to lint than that made on a fourdrinier machine. [2],[3]

The overall amount of filler in the sheet is also linked to the filler linting propensity. The higher the filler content, the more likely the filler will deposit as lint. [10]

Printing Tests

There has been significant research in the field of designing printing experiments to artificially remove fibre and filler from the surface of machine made newsprint or paper. Traditional laboratory based tests such as the IGT pick test and Prüfbau wet pick have been used extensively. [5],[7],[9]

Mangin and Dalphond [7] evaluated three force intensities corresponding to dusting, linting and picking, using an IGT printability tester at constant (2.5 ms^{-1}) speed.

Lindem and Moller [9] report that no relationship could be found between the IGT test result and the quantity of lint accumulated on the commercial printing press blanket. The IGT is proposed as being more suited to measuring internal bond strength than it is in assessing loosely bound material on the paper surface.

Similarly, no relationship could be found between the Prüfbau wet pick test and the quantity of lint accumulated on the commercial printing press blanket.[9]

Heintze and Ravary [8] warn that laboratory tests that print only a small area of the paper should be used with caution since the actual material removed in these tests may be very different from the material that builds up on the blanket of the commercial offset press.

Ionides [3] warns that in laboratory tests, due to the small sample area, in order to get a significant amount of lint to measure, the stress applied to the sheet surface must be greater

than that encountered on a commercial offset press. This may make the test procedure unrepresentative. [3]

Most linting studies concentrate on the lint accumulated on the offset blanket, but linting is a problem that affects the entire press, including the ink train and rollers [8]. This is an area where it is difficult to replicate real world conditions on a laboratory scale printing test.

Some linting studies have been conducted on commercial printing presses to examine the conditions that produce linting. [9],[12].

Lindem and Moller [9] carried out a series of 27 printing trials under standardised full scale production conditions on a four-colour offset press in Norway. The principle aims were to :

- Evaluate the effect of blanket lint deposits on print quality
- Establish the nature of the lint and where it deposited on the blanket
- Measure the quantity of lint deposited
- Identify simple laboratory methods that could predict quantities of lint deposited on the blanket with reasonable accuracy.

Lindem and Moller [9] found that the majority of lint consisted of ray cells and fibre fragments from reaction wood. This lint did not result in any marked deterioration in print quality after 100,000 copies were printed and so could not be regarded as being a problem. For those samples that showed the highest amount of linting, the lint consisted of fibrillated fibrous material in addition to the ray cells and fibre fragments. Generally, linting occurred more in unprinted regions than printed regions. Lindem and Moller [9] were unable to find a

lint predicting method that corresponded to the amount of lint deposited on the actual offset blanket.

Wood et al [12] found that commercial scale printing trials could be used to demonstrate significant differences in the linting of a series of newsprint sheets. A correlation was found between the linting in cold set offset and heat set offset. Press variables were found to have a major effect on the linting propensity of the newsprint.

Whilst the commercial printing trials are able to give an indication of linting in the pressroom, conducting trials is often difficult due to competition between production and research based priorities.[3],[13]

As a proactive measure, paper mills began conducting their own version of commercial print trials by evaluating linting propensity on small pilot offset presses for audit or quality assurance purposes. For example, the Apollo lint test is performed on a small web fed offset press and is commonly used in the Canadian newsprint industry.[7]

Norske Skog, Boyer Mill uses a Heidelberg GTO-52 offset press as a laboratory test to measure the linting tendency of newsprint and to study the factors affecting print quality.[14]

It was found that for every ink setting studied, the more excess fountain solution that was available, the lower the linting tendency. Unfortunately optimum print density was associated with high levels of linting.[14] Increasing fountain solution is believed to decrease linting due to emulsification within the ink, which decreases viscosity and tack.[2]

Earlier theories that the fountain solution weakens hydrogen bonds in the paper and subsequently increases linting do not appear to be valid.[9]

Despite the attempt to replicate the commercial print environment, researchers believe that that pilot press testing is not satisfactory. Mangin and Dalphond [15] have noted that the linting propensity of paper is the result of an interaction between the paper linting propensity and the press parameters. It is concluded from this that measuring lint accumulation on the blankets of a pilot offset press is not a good test to evaluate the linting propensity of paper, since it can not replicate the conditions in a large commercial press room.

It has also been concluded by Mangin and Dalphond [7] that a group of papers tested on two different offset presses, or on the same offset press, but under different conditions may not rank in the same order for linting propensity. It is suggested that testing the paper linting propensity on an offset press is limited to the type of press and printing conditions used.

Mangin and Dalphond [7] suggest that the linting propensity of paper should be considered as the response of the paper surface to different forces. These forces will be different on any given press, run under any given condition. Similarly researchers [2],[4] propose that fibres are removed from the surface of the paper when the external forces exceed the forces holding the fibres together in the network.

Ionides [3] proposes further that the force that removes lint in the offset press nip is a force perpendicular to the sheet surface, compared to the frictional forces that loosen up the lint which are parallel to the sheet surface and scuff the paper in the nip.

Printing press variables that have been assessed for their effect on linting include [1],[2],[16]

- Printing Speed
- Pressure
- Temperature and Humidity
- Length of printing run
- Nip / Blanket packing
- Take-off geometry
- Plate to Blanket
- Blanket age
- Cleaning solvents
- Hard vs compressible blankets
- Printing Form / Density
- Ink weight
- Ink Tack / Rheology
- Fountain solution
- Wetting agents
- Hydrophilic correctors

Some of these variable are discussed below.

Printing Speed

It is generally accepted that linting increases with printing speed. [1],[2] This increase in lint accumulation varies inversely to the diameter of the blanket cylinder.[1] The printing speed also affects the size of particles removed.[1],[2] An increase in speed increases the size of lint particles.[1]

Pressure

There are conflicting reports on the effects of pressure. Some research indicates that linting increases with increasing pressure and the opposite findings are reported in other research work. [2] There is a lack of comprehensive models of ink-paper-press interactions to predict the effects of printing pressure. [1],[2]

Temperature

As temperature increases, the tack and viscosity of the ink decreases. This causes the ink transfer to be smoother and thus decreases linting. [2]

Length of Printing Run

The accumulation of lint in a press is not uniform between printing units. There is more linting in the first unit of the press and the lint consists of particles that are not bonded to the surface. [2] Subsequent printing units have lint that is weakly bound into the sheet. The stronger the binding force of the lint, the later in the printing process it is removed. [2]

Bonding can also be adversely affected due to moistening of the sheet. This is sometimes referred to as water induced linting.[2] The longer the printing run, the more the total lint quantity increases. Because a large quantity of the lint travels back up the process to the ink train, the ink quality will decrease during the printing run.[2]

Blanket Effects

The ideal set up of the press has the two cylinders which form the nip packed evenly. Mis-matching the packing increases the likelihood of linting. [2] Mis-matching is common because press operators routinely change individual blankets when necessary, instead of changing them together, which results in an inevitable mis-match because the new blanket has not packed down as much as the older one. [2] Overpressure has been reported to reduce linting, however as overpressure also decreases print quality and reduces the life of blankets and plates, it is not often used to reduce linting. [13]

Older press blankets cause more linting than new press blankets due to a layer that has accumulated during its working life despite being routinely cleaned to remove such buildups. [2]

Cleaning solvents can make the blanket swell and increase in roughness and thickness. This subsequently can increase linting. [2]

Lint accumulation differs between hard and compressible blankets. On a compressible blanket, lint decreases with decreasing print density. On a hard blanket, lint does not vary significantly with density. [2] There are conflicting reports of which blanket types create more linting. [2]

Take-off Geometry

In normal offset printing, the nominal take off angle is 15° . In general, the paper side printed at the nominal take-off angle, partially wrapped up on the blanket cylinder causes less lint accumulation than the opposite side. [1][2]

Web feed, web tension

Web tension affects the linting propensity as it affects the true take-off angle of the paper. [2]

Printing Form

Linting increases with print density, due to more ink coverage and more ink film to surround and grip the fibres. [2] The highest lint accumulation is usually in the halftone areas. The lint is considerably less in the solids and non-image areas of the print. [1],[2]

Ink Weight

The effect of ink film thickness on deposit of lint on the blanket seems negligible. [1],[2]

Ink Tack and Viscosity

In general terms, the literature states that an increase in ink tack increases linting. An increase in ink viscosity increases linting. [1],[2]

Fountain Solution and additives

In offset printing, fountain solution is not only transferred in non image areas , but also in image areas as it is emulsified with the ink. [1],[2] The fountain solution thus decreases the tack and viscosity of the ink and thus causes the linting to decrease. Mangin [1] found that increased dampening decreased linting in the first station, but had no affect on succeeding printing units. The addition of alcohol to the fountain solution decreases lint. However, most newsprint presses currently work without alcohol.

The addition of hydrophilic correctors, which prevent corrosion in the printing plates, decreases accumulation of lint on the blanket. [2],[13] However, the dislodged lint still travels around the press. [2] Increasing the hydrophilic corrector content forms a slip layer on the blanket which prevents the lint from leaving the paper surface or inhibits its

deposition. [13] The hydrophilic corrector does not evaporate ;it forms a moist lubricating layer on the blanket surface. [13]

Paper variables

Paper machine variables are also an obvious influence on the linting propensity of paper. Stock preparation, furnish, forming, wet end chemistry, pressing, drying, calendaring and slitting can all potentially affect the propensity of a paper to lint.[2] When traditional fourdrinier machines were upgraded to twin wire assemblies, the linting tendency decreased.[3],[8] When the press sections were upgraded, the linting tendency also decreased.[9],[12],[16]

Fractionating the pulp using hydrocyclones and then refining the rejects reduces linting and improves the surface properties. [2] Generally screening has little effect on linting as the fibres are separated based on size / length, not on specific surface. Centricleaners or hydrocyclones do a more effective job of removing fibres with a low specific surface because this is the basis on which they separate. [2] The reject rate can be controlled to improve the linting propensity of a paper grade.

It is proposed that the presence of filler in the sheet can increase the linting tendency because the filler particles settle between the particles and prevent the hydrogen bonding that connects the fibre matrix. [2] Filler particles are likely lint candidates as they are poorly bound in the sheet.

The use of de-inked stock can induce the linting of the filler from the de-inked pulp. The filler is attracted to the resin on the resin rich ray cells and then travels to the blanket with the ray cells. [2],[13]

As the printing run proceeds, the amount of filler as a percentage of the overall lint actually decreases, because the filler is the first to deposit on the blanket. [2]

Newsprints with a high waste percentage are reported to lint less. This may be attributed to less ray cells in the furnish, as ray cells are the predominant constituent of fibrous linting. [2] The higher proportion of kraft fibres from magazines also contributes to fibre bonding.

Pulp coarseness, defined as weight per unit length of fibre affects linting. The higher the fibre coarseness, the higher the linting propensity of the paper, due to less overall sheet bonding. [3] Refining of pulps to produce well developed fibres decreases the linting propensity of paper. [3]

For paper made on a Fourdrinier, the linting propensity of the top side of the sheet is 20–60% more than the wire side of the sheet. [3] This is due to the fines distribution in the sheet, with more fines trapped on the wire side of the sheet. The fines provide multiple bonding sites in the paper structure. Also, potential lint candidates such as ray cells and stiff fibres or shives are removed during drainage on the bottom side of the fourdrinier. [3] The conclusion therefore is that gap forming produces a paper with decreased linting propensity on the top side of the sheet as compared to a fourdrinier. [2],[3]

Since the material collected at press roll doctor blades closely resembles that collected from offset printing blankets, any efforts to reduce press section picking, would also decrease the linting propensity of paper. [2] Higher press loads and a gentle transfer out of the press section decrease the linting propensity of a paper. [2],[3] Suction presses which remove water and loose surface fines also decrease linting, by removing the linting candidates from the surface of the sheet. [3]

As in the press section, picking can also occur in the dryer section of a paper machine. Having the drying cylinders too hot is a common problem that results in picking and hence increases the linting propensity of papers. [2] A steady increase in temperature through the early stages of the drying train are preferred for reducing linting. [3] Whilst calendering consolidates the sheet structure, it does not necessarily decrease linting. Hard nip calendering at low temperature actually increases linting, while temperature soft nip calendaring can decrease linting. [2] Calendering at too high a load can increase linting by weakening the sheet. [3]

Offset blankets sometimes have a line of linting on the edge of the paper path. This can often be attributed to slitter dust. This can be eliminated at the paper machine winder / sheeter by vacuum extraction of edge / knife dust. [2]

The linting tendency of papers themselves should have decreased as technology has improved with paper machine upgrades and the manufacture of new paper machines throughout the world. This may be the case, but the increase of offset printing in the newsprint industry [2-5] and higher quality expectations than ever before have resulted in

linting being an important problem in the printing industry. This is magnified by the change from black to multi-colour printing of newspapers and the dramatic increase of printing press speeds over time.[12] The use of multi-colour printing has increased linting due to the addition of ink and fountain solution in multiple consecutive stations which weakens the fibre bonding of the paper surface.

Characterisation and quantification of lint

There have been numerous approaches to quantify lint accumulation during printing which include [5],[8] :

- Lint removed from press blanket with adhesive tape and fibres counted visually or by image analysis
- Molten wax poured on offset blankets and cooled to trap the lint and ink. Subsequent filtration of the molten wax and treatment with a solvent separates the lint from the carrier.
- Lint removed from the press blanket with adhesive tape and quantified with caliper measurements
- Lint removed with the Domtar lint collector and then filtered. The Domtar lint collector is a tray, which is held firmly against a stationary offset blanket area to be sampled. Using dilute isopropanol and a brush the lint and ink is washed off the blanket into the tray and bottled. These bottled samples are then screened to determine the mass fractions retained on each mesh and may also be subjected to visual analysis. [17]
- Lint characterized by Kajaani fibre length detector.
- Colour / Brightness measurement taken of offset press blanket after passing paper sheets through and compared to the clean blanket

The lint removed from an offset blanket ranges in size from very fine fibre and filler fragments, ray cells, whole fibres to mini shives and other debris.[4],[8-9] Whilst image analysis can be used to quantify the produced lint [16], it is important to note that the single large particles often cause more printing problems than an equivalent area of small ones. [3]

In years gone by, newsprint lint consisted mainly of large mechanical pulp fibres, which were loosely bonded into the paper surface. Advances in fibre development within the pulping process have been able to solve this issue.[12]

The current trend is more towards lint deposits of small ray cells, other fines and fillers.[2],[4-5],[13] The common feature of these particles is that they are short, stiff and have a low specific area which means that they have low bonding potential into the sheet of paper.[3-5],[9],[12] Nearly all lint particles are shorter than 1mm with over 90% reported as being less than 0.3 mm long, including ray cells which are typically about 0.1 – 0.2 mm long.[9],[13] The disadvantage of the smaller lint particles is their mobility in the printing press, traveling up into the ink train or fountain solution unit.[15]

Going back to the source, researchers [4-5] suggest that the linting propensity of paper be controlled by decreasing the linting propensity of the base pulp by optimizing the mechanical pulping process. Processes such as screening, centri-cleaning, reject refining, chemical treatment were considered in order to deliver a pulp with decreased linting tendency to the paper machine.

Measurement of filler distribution in paper

The use of scanning electron microscopes to determine filler content in paper structures has been reported[10],[18-20]. Cross-sections are prepared by microtoming and embedding the paper into an epoxy resin block for examination. [10],[18] Surface samples are simply placed on a stub and then into the microscope.

Elemental analysis has been conducted with energy dispersive spectroscopy to produce elemental maps of the paper, using a scanning electron microscope (SEM).[18-20]

Alternatively back scattered electron imaging can be employed, which takes advantage of the atomic number differences of the material.[18] The details of this method are explained in Section 3.2.1.2.

Failings of these types of methods is that only small areas are measured and these may not fully represent significant structural features in the paper such as sheet density distribution, microformation, pores and wire marks. [18]

Other issues include the length of time required to prepare the samples by microtome and the limit of SEM technology to 1000X magnification.[18]

The need for more information on how to quantify filler in paper samples is one of the main drivers for this project and body of work.

3.0 EXPERIMENTAL

3.1 Printing Experiments

3.1.1 IGT Testing

The IGT Printability Tester AIC2-5 Series 414.Z at the National Printing Laboratory, Department of Chemical Engineering, Monash University was chosen for the laboratory printing experiments as it is used as a preliminary indicator of linting at Norske Skog, Tasman Mill, NZ.

Details of the procedure used at Norske Skog Tasman Mill and the National Printing Laboratory may be found in Appendices A and B respectively.

Two papers of known linting propensity, one high and one low, were sourced from Norske Skog, Tasman Mill to establish the set of variables on the IGT Printability Tester which duplicated the known linting propensity of the paper samples.

The following variables were changed in order to establish the correct settings for the IGT Printability Tester.

Variable	Range Tested	Units
Ink Volume	0.1 – 0.35	ml
Ink Film Thickness	2 – 8	µm
Constant / Acceleration mode	Constant and Acceleration modes	
Printing Speed	1 – 7	ms ⁻¹
Printing Nip Pressure	625 – 800	N
Ink	IGT Picking Test Ink, normal tack, 408002 IGT Picking Test Ink, high tack, 408003	

Table 3.1 – Variable ranges considered in setup of IGT Printability Tester

Appendix C shows the experimental matrix considered while developing the settings for the IGT experiments. The ink volume of 0.7 ml, previously used for hand sheet experiments by R. Koehly [10] was inappropriate and excessive for the machine made paper. This is due to the lower surface roughness of the machine made paper compared with the hand sheets. An ink volume that gave sufficient print density and covered the test sample in sufficient ink was chosen.

The constant speed setting allowed for a larger region of analysis and was chosen as the preferred setting. Limited linting / picking was achieved at lower print speeds, so a print speed was chosen where linting was definitely occurring on the high linting sample and hardly occurring on the low linting sample

The experiment was not overly sensitive to printing pressure, so an upper pressure setting was chosen to ensure sufficient pressure in the nip to give adequate ink coverage.

Experiments in ink tack showed a significant increase in linting / picking when the high tack ink was used. However, the high tack ink was unable to distinguish between the high linting paper and the low linting paper under most conditions. For this reason, the normal tack ink given in Table 3.1 was used.

After a series of experiments, it was concluded by visual analysis that the following set of variables was most appropriate for determining the linting propensity of newsprint. This is the set of variables that showed considerable linting on the high lint paper and low linting on the low lint paper.

Variable	Setting	Unit
Ink Volume	0.2	ml
Ink Film Thickness	5	μm
Constant / Acceleration mode	Constant speed mode	
Printing Speed	4	ms^{-1}
Printing Nip Pressure	800	N
Ink	IGT Picking Test Ink, normal tack, 408002	
Printing Disc	50mm wide, covered with coated rubber 80 Shore A	

Table 3.2 – Variables for setup of IGT Printability Tester

Table 3.3 shows the variables used by Norske Skog Tasman Mill. Appendix A has the full set of procedures for the test conducted at Norske Skog Tasman Mill.

Variable	Setting	Unit
Ink Volume	0.15	ml
Ink Film Thickness	3.6	μm
Constant / Acceleration mode	Constant speed mode	
Printing Speed	2.5	ms^{-1}
Printing Nip Pressure	625	N
Ink	Sicpa stable high tack ink (11056096)	
Printing Disc	50mm wide, covered with coated rubber 80 Shore A	

Table 3.3 – Variables for setup of IGT Printability Tester at Norske Skog Tasman Mill

Although pick tests are usually conducted under accelerated speeds, this series was conducted at constant speed, which is supported by literature. [7] Norske Skog Tasman Mill also conducts the test under constant speed.

The printing speed, printing pressure and ink volume vary slightly between the experiments conducted and the procedure at Norske Skog, Tasman Mill because the ink differed between the two. The experimental test conditions used for the work in this theses were selected to

replicate the results of the Norske Skog test by producing high lint on the high lint sample and barely any lint on the low lint sample.

Six unique samples of newsprint branded Image / Norstar from Norske Skog, Boyer Mill were tested on the top side and bottom side with 3 replicates for each sample. These samples were submitted for analysis by Norske Skog, Boyer Mill based on interesting results that had been obtained from their own internal mill quality and audit testing.

Sample Number	Boyer Roll Number Reference
B1	B0069368
B2	B0074346
B3	B0067718
B4	B0076485
B5	B0076570
B6	B0069624

Table 3.4 – Paper sample references

When the Printing disc has been inked and printed, there is residual ink on the printing disc. The IGT Printability Tester manual indicates that a calculation can be made to determine the amount of ink which has been removed and then this amount can be added to the inked up printing disc to start a new experiment. This approach was tried but found to be unsuccessful as the results obtained did not correlate well with those obtained from freshly cleaned printing discs. Due to this, the author advises that clean, uninked printing discs be used for each print run on the IGT Printability Tester.

In addition to performing the printing experiments, the paper samples were weighed before and after printing to determine the amount of ink applied to the surface of the sheet. This was calculated as 2.4 gm^{-2} (Appendix D), for the conditions described in Table 3.2. The ink

applied to each sample was consistent, with a standard deviation of 0.1 gm^{-2} . An alternative method of calculating the ink applied, would be to weigh the inked printing disc before and after printing.

All experiments were conducted in the constant printing speed mode. It was noticed in the printed IGT paper samples that there was a degree of acceleration, even in this mode of operation as the amount of lint removed on the sample increased from start to end of printing. This was apparent in all samples. This is clearly seen in Figure 3.1



Figure 3.1 – More lint removed in latter part of IGT Printed samples, despite constant printing speed

Care must be taken that printed sheets are dry before further analysis is performed.

The time taken to set up equipment and samples for testing of 4 samples is 45 minutes. This includes the time taken to clean the inking equipment prior to testing of subsequent samples.

3.1.2 Quantification of Lint Removed

3.1.2.1 Image Analysis of Printed Paper

The 36 samples of paper (6 samples x 3 replicates for top and bottom) were analysed for area of lint removed by image analysis

The first series of experiments used an optical microscope with a 50 X magnification and camera to capture images of the surface of the paper. This method proved inappropriate due to the surface roughness of the paper and non-homogeneous ink coverage on the paper at this micro level.

At this magnification, it is difficult to distinguish between linting of fine / filler material and the effects of incomplete surface coverage. This can be seen in Figures 3.2 and 3.3 in the regions labeled 1 and 4. Regions labeled 2 and 3 are clearly that of fibre lint. The scale markers represent 500 μm .

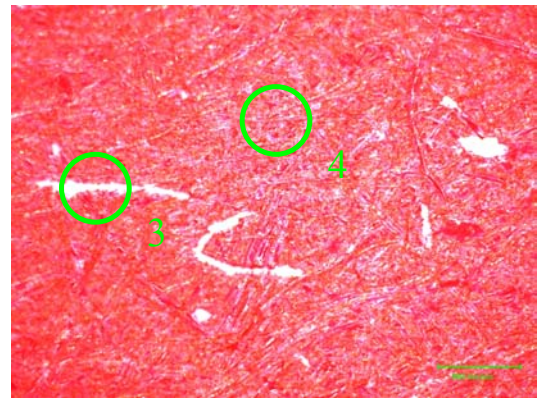
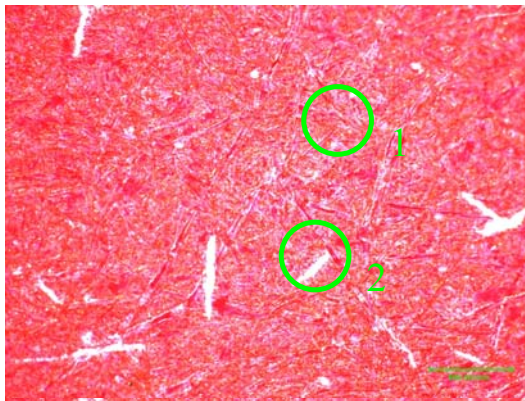


Figure 3.2–Image of IGT Printed Paper–50X Figure 3.3–Image of IGT Printed Paper–50X

An alternative method of capturing the images of IGT Printed paper was sought. A Hewlett Packard Scanjet 6300C Flatbed scanner was used to capture the images. A 1: 1 image was captured (sized 4.8 x 10 cm) at the bottom of the printed image as this represented the area of most lint removal. This is shown in Figure 3.4

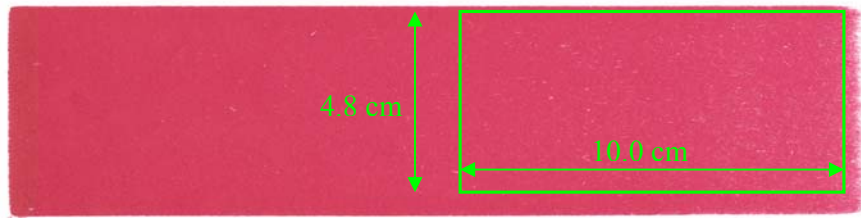


Figure 3.4 – Image captured of printed IGT sample

The images were then analysed by image analysis software, Image Pro Plus, to determine the size distribution of non- printed areas. Figure 3.5 shows the original image. Figure 3.6 shows the areas that have been darkened and then counted as lint by the image analysis software.



Figure 3.5 IGT Test Print 1:1



Figure 3.6 Image analysis quantification

The settings used were Hue : maximum (255), Saturation (94), Intensity : maximum (255)

The particles were counted in three separate bins and then averaged for each duplicate. The full data is reported in Appendix E.

Fines / Filler	0 – 0.05 mm ⁻²
Small Fibres	0.05 – 0.1 mm ⁻²
Fibres	0.1 - 10 mm ⁻²

This method proved to be more representative of the lint that was visually seen on the IGT test prints. This method also allows for a larger area of sample to be considered which is preferred.

3.1.2.2 Image Analysis of Lint

Experiments were conducted to view the type of lint that had been removed from the paper surface during the IGT Printing experiments.

Prior to printing, the printing discs were thoroughly cleaned in a beaker of heptane, in an ultrasonic cleaner for 10 minutes. This ensured that any debris (fibrous, filler or from the cotton rags used to clean the discs) was not present.

After each test print on the IGT printability tester, the printing disc was immersed in a fresh solution of heptane and placed in an ultrasonic cleaner for 10 minutes. This removed the accumulated lint debris from the printing disc.

A methyl violet dye was added to the heptane solution to stain the lint particles. The entire solution was then passed through a vacuum assisted filtration process to separate the carrier solution from the lint particles. Several passes were conducted through the filter (5 μm) to ensure that all lint particles had been collected.

The filtrate was discarded and the lint remaining on the filter paper was analysed under optical microscope as shown in Figures 3.7, 3.8, 3.9 and 3.10.

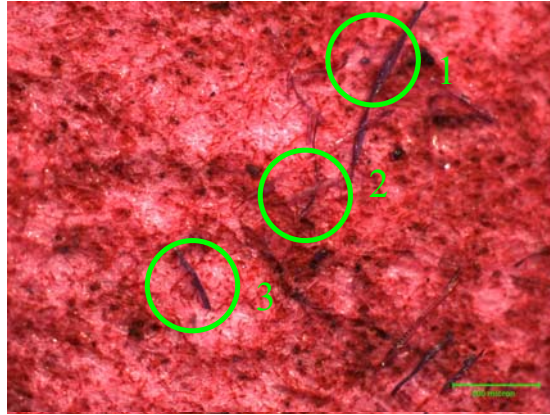


Figure 3.7 – 50 X View of lint debris. The scale marker represents 500 μm .

Regions 1 and 3 in Figure 3.7 clearly show the dyed fibrous lint particles. Closer inspection of the image reveals that some fibrous lint particles, such as that shown lying horizontally in Region 2, are not dyed. The red region in the background is the test ink that has been washed from the IGT printing disc.

Whilst it would be straightforward to conduct image analysis on the filtered lint sample, the results would not be accurate unless all lint particles (fibrous and filler) were stained with the dye, so as to differentiate the lint from the filter medium and ink in solution.

Various methods were used to try and achieve this such as adding the dye at the end of the filtration process, directly onto the filter media, but the same problem persisted.

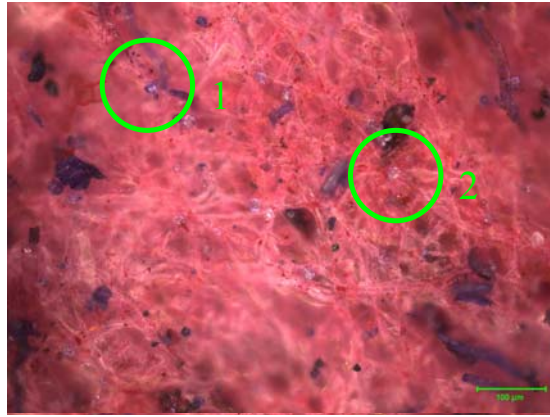


Figure 3.8 - 200X View of lint debris. The scale marker represents 100 μm.

Under a higher magnification it can be seen that non-homogeneous dyeing of lint material is also occurring. Region 1 in Figure 3.8 clearly shows a particle that has been dyed. Region 2 in Figure 3.8 clearly shows a very similar looking particle that has not been dyed. Any visual analysis conducted on such a sample would not be accurate.



Figure 3.9 – 50 X View of lint particles, including a cotton fibre. The scale marker represents 500 μm.

Figure 3.9 clearly shows a cotton fibre in the image. The origin of this cotton fibre is most likely from the rags used to clean the IGT Printability test equipment. It is important to ensure that adequate cleaning of the printing disc takes place prior to any experimentation.

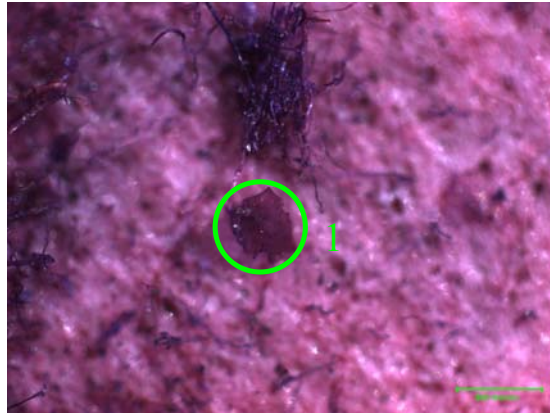


Figure 3.10 – 100 X view of lint particles, including residual ink. The scale marker represents 500 μm .

Region 1 in Figure 3.10 clearly shows a particle of unknown origin that was later identified by FTIR (Norske Skog, Boyer Research Centre) as a piece of ink. In order for image analysis to be conducted accurately on any samples of collected lint, it is important to identify all sources of contamination and remove them.

A clearer differentiation between background ink and dyed lint particles would be obtained if the printing ink was replaced with a clear IGT picking test oil. This would not have replicated the method of lint testing used in this experiment set, as ink was used exclusively to cause linting on the test strips .

In addition, a method was never found to be able to dye all of the lint particles adequately, so as to differentiate from the background filter medium. For these reasons, this technique is not

recommended for the characterization of lint particles and is not used in the results presented in this thesis.

3.1.3 Heidelberg Print Tests

Norske Skog (Boyer Mill) conducts audit testing and quality testing on newsprint by way of a Heidelberg Lint Test.[14] Heidelberg lint is quoted as the amount of lint (gm^{-2}) deposited on an offset press blanket, on a 50 % screen area, after a print run of 7,000 sheets on a Heidelberg GTO52 offset press.[20] It has been noted in literature [1],[2] that the highest lint accumulation is usually in the halftone areas.

The quantity of lint is assessed by weighing adhesive tape strips that are adhered to the blanket and then removed, picking up the deposited lint. [13] Any value greater than 5 gm^{-2} is considered as high, $3 - 5 \text{ gm}^{-2}$ is average and less than 3 gm^{-2} is low. The ink used in this test has a tack of 13 and a densitometer is used throughout the run to ensure that the density of the print is kept close to its target of 0.70 in the full screen area.[13]

The test pattern for the Heidelberg lint test is shown in Appendix F.

Of particular interest is a phenomenon noted by Norske Skog, Boyer Mill. In an area of the test pattern depicting trees, lint often accumulates in a region along the top of the tree line as depicted in Figure 3.11.



Figure 3.11 - Detail of Norske Skog Heidelberg Test Print. Full print shown in Appendix E.

At times the accumulation of lint across the top of the tree line is broad and at other times it is a narrow band of lint accumulation. Microscopic analysis by Norske Skog Boyer has concluded that when the band of lint is broad, the lint is mainly fibrous. When the band of lint is narrow, the lint is mainly filler.

3.2 Filler Size Distribution

Several techniques were trialled to quantify filler size distribution and area in paper surfaces. The development of these techniques is described in this section. During the time available it was not possible to obtain quantitative information for all techniques. However all trials have been included so as to give a starting point for future work.

3.2.1 SEM Backscatter

The aim of the SEM / backscatter experiments were to :

- obtain images of the paper surfaces, top and bottom
- analyse the images to quantify particle size distribution of the filler in the paper surface.

3.2.1.1 Sample Preparation

The paper samples listed in Table 3.4 were cut with a razor knife to 1 cm x 1cm square.

These paper samples were mounted on stubs with double sided adhesive tape.

A small amount of carbon was applied with a brush to the corner of the sample to earth the sample to the stub. The sample was then coated with carbon in a Dynavac CS300 sputter coater with an aim coating thickness of 240 angstroms. This final coating is to make the sample electrically conductive.

The samples were then ready for use in the microscope.

3.2.1.2 Microscopic Analysis

A Phillips XL30 Field Emission Scanning Electron Microscope, located at CSIRO, Forestry and Forest Products, Clayton, Vic. was used for the microscopic analysis.

The stubs were mounted securely onto a carousel, which in this case carried six unique samples. Air was evacuated from the chamber and the microscope set up with the desired variables to view the samples.

The SEM produces electrons that impinge on the sample. A variety of signals can be captured due to interaction of the impinging electrons with the sample :

- Secondary electrons
- Backscatter electrons
- X-rays

There are different interaction volumes for each signal, as shown in Figure 3.12.

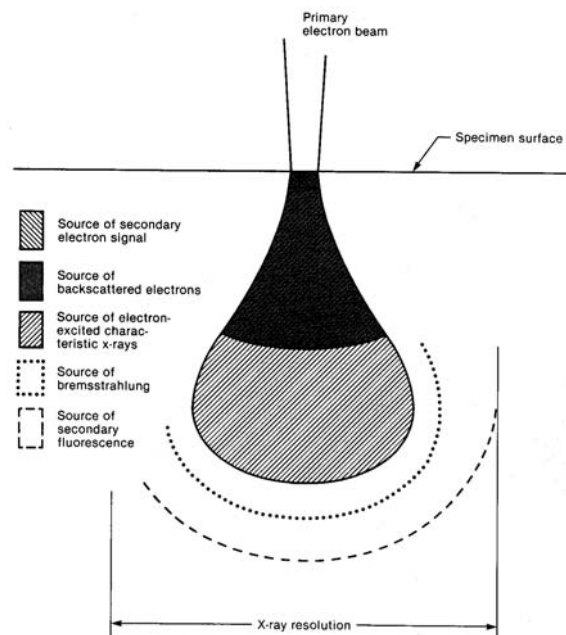


Figure 3.12 Illustration of interaction volumes for electron/sample interactions [21]

The popularity of SEM is partly due to its ease of operation. It is very sensitive to low concentrations, is non destructive and requires minimal sample preparation. [21]

Secondary Electrons

Secondary electrons are the electrons that escape from the sample when the primary electron impinges. [21] Secondary electrons are more commonly known as any secondary electron that is less than 50 eV in energy.[22] These secondary electrons with little energy can only be detected if they are created near the surface of the sample. [21]. For this reason it is very important that the sample is flat on the stub.

The greatest density of secondary electrons is created by the primary beam before it has a chance to spread and therefore the spatial resolution is very high. The topographic sensitivity and high spatial resolution make secondary electron images very popular for micrographic images such as that shown in Figure 3.13.[21] Secondary electron images are not able to differentiate consistently between the filler and fibre particles in a paper sample as they do not carry information on elemental composition of the sample.

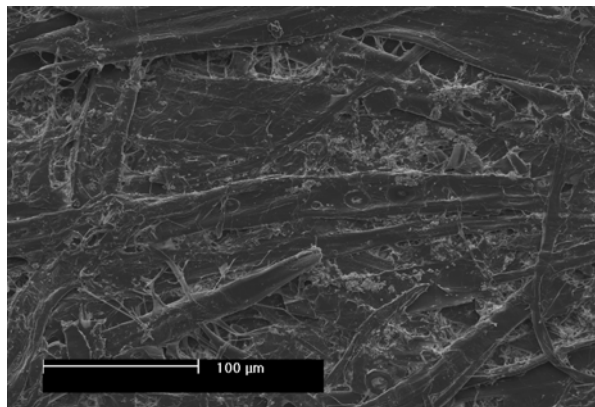


Figure 3.13 - 250X Secondary Electron image of B1 bottom side

Secondary electron images were obtained for each of the 6 samples analysed on the top and bottom surfaces. These images were taken as reference images only. No further analysis was undertaken with these images.

Backscattered electrons

If the primary electron interacts with the nucleus of the sample atom, an electron may scatter in any direction with little loss of energy. This electron is known as a back scattered electron and is much more energetic than a secondary electron. It is generally more than 50 eV in energy. [22] and can come from a greater depth in the sample. Because of the increase in the depth over which backscattered electrons are generated, the backscatter technique will have a lower spatial resolution than can be obtained by measuring secondary electrons.[21]

However, due to the fact that backscattered electrons interact with the nucleus of an atom, they are able to distinguish between differences in atomic number. The higher the atomic number in the sample, the greater the positive charge of its nucleus and the more likely that an electron will produce a backscattered electron. [21]

The clay filler in the paper sample is $\text{Al}_2\text{Si}_2\text{O}_7$. Aluminium and Silicon have an atomic number of 13 and 14 respectively. The carbon in the cellulose has an atomic number of 6. It can be seen in Figure 3.14 that the aluminium and silicon atoms (in the filler) produce a strong backscatter signal, thereby enabling the differentiation between filler and fibre in the paper sample.

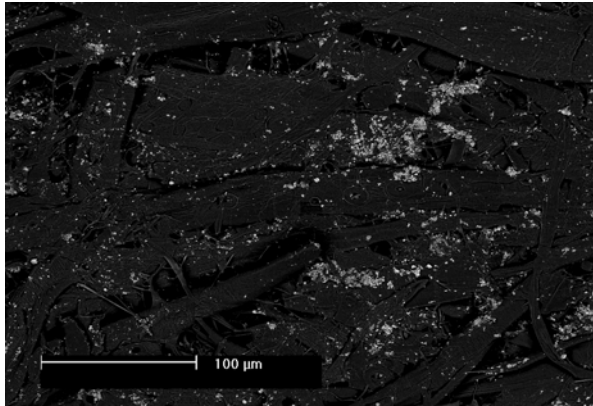


Figure 3.14 - 250X Back Scattered Electron image of B1 bottom side

Back scattered electron images are able to differentiate between elements if the atomic number differs by more than 3.[22] This is why there is such a good differentiation between the filler (Al and Si) and the fibre (C). There is no differentiation between the Al and Si, since they are only one atomic number apart. This is useful for our analysis as it allows the clay particle / agglomerate to be grouped as a whole.

The set up for the SEM in backscatter mode is very sensitive, with numerous variables to be considered before specifying the correct set up for a particular experimental set. Sub-optimal setup of the SEM may result in sub-optimal images for subsequent image analysis. The quality and accuracy of the image obtained is paramount.

Substantial time and effort was therefore committed to this part of the experimental work, to obtain the optimal settings to conduct the experiments under. The following settings were used for the work conducted in back scatter mode.

Variable	Setting
Accelerating Voltage	5 kV
Spot Size	5
Working Distance	10.5 cm
Brightness	34.6 %
Contrast	95.9 %
Magnification	250 %

Table 3.5 – Settings for SEM Experiments

Twenty back scattered electron images were obtained for each of the six paper samples, top and bottom, totaling 240 images in all.

X-Rays

The source (primary) electron ejects an electron from an inner shell of a sample atom. The resulting vacancy is then filled by an electron from a higher-energy shell in the sample atom. In dropping to a state of lower energy, the vacancy filling electron must give up some of its energy. This energy appears in the form of electromagnetic radiation (an x-ray) and is equal to the energy difference between the two electronic levels involved. Each element in a sample, when subjected to the bombardment of electrons will emit a unique and characteristic pattern of x-rays. [21]

X-Rays generated from electron transitions in atoms are particular to an element due to characteristic energies associated with the x-rays. In this way, theoretically x-ray analysis from the SEM could be used to differentiate between the filler (Al and Si) component and fibre (C) component of the paper sample.

X-Rays however, travel much greater distances through the sample than the secondary or backscattered electrons and as a result, the spatial resolution is less.[21]

An illustration of the interaction volumes for electron / sample interactions is given in Figure 3.12 [21]. It shows why x-rays have the poorest resolution, as they come from deepest within the sample.

Experiments were conducted to obtain images of the paper sample by x-ray detection. The resolution was not high enough to show agglomerates of clay known (by back scatter detection) to be within the sample. Images from the x-ray maps were compared to the back-scattered electron images and the resolution of the x-ray map was inferior, displaying small discrete areas of detection of Al and Si, as opposed to the well defined filler vs fibre separation obtained in the back-scattered electron images. Figure 3.15 shows the x-ray detection image, accumulated after 2 hours of scanning. The image is not suitable for image analysis as the filler aggregates can not be seen.



Figure 3.15 – X-Ray Map of surface of paper sample

Further experiments were conducted, capturing data over a longer time frame. The original back scattered image is shown in Figure 3.16. Figure 3.17 shows the image with Aluminium mapped. This is a blurred replica of the image acquired with the back scatter detector.

Figure 3.18 shows the aluminium and the silicon mapped. This image shows improved clarity over Figure 3.17, which shows aluminium only, but it is still inferior to the back scatter image in Figure 3.16. The data acquisition took place over 15 hours and was taken at a magnification of 250 % and 10 keV beam current.

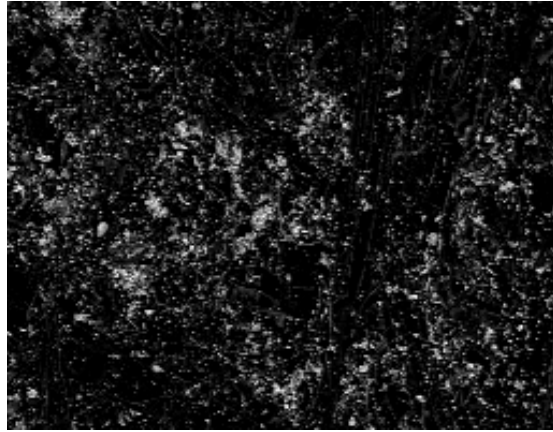


Figure 3.16 – Back Scatter Image of B3 Top

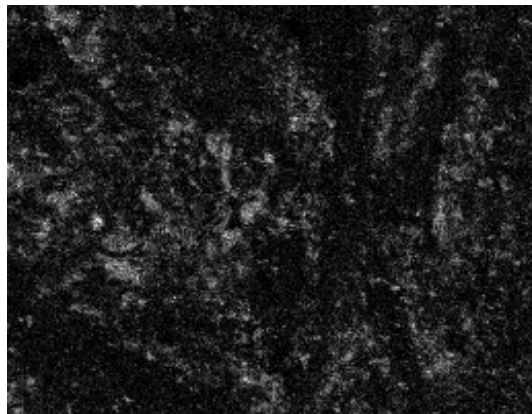


Figure 3.17 – Aluminium X-Ray Map of B3 Top

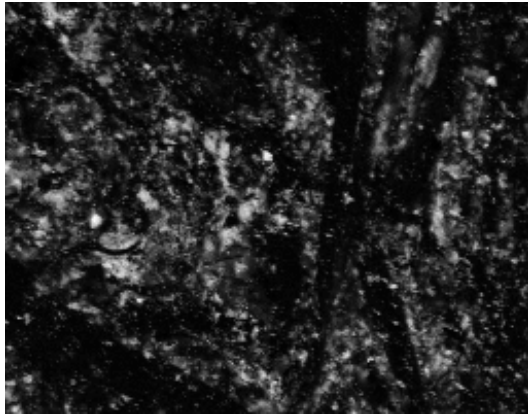


Figure 3.18 – Aluminium and Silicon X-Ray Map of B3 Top

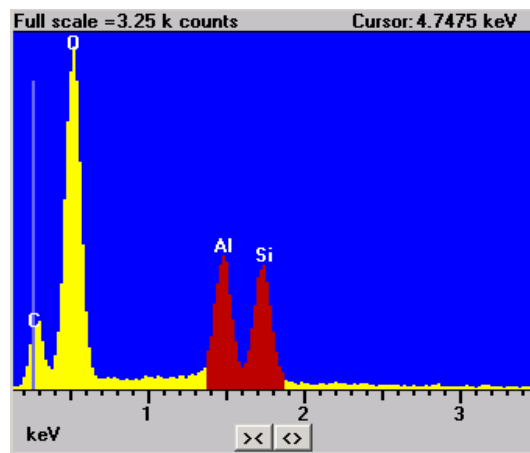


Figure 3.19, Spectrum of x-rays detected in B3, top

Figure 3.19 shows the spectral peaks of Carbon, Oxygen, Aluminium and Silicon, all found in the paper samples. The excitation energies are as follows: Al (1.487 keV), Si (1.74 keV), O (0.525 keV), C (0.277 keV).

Of the three techniques investigated using the SEM, only the back scatter and x-ray can distinguish between filler and fibre. The x-ray technique suffers from poor resolution and the

long time required to capture a single image. Therefore the back scatter technique was chosen for the next step in the experiment – quantification of the filler particle distribution by image analysis.

3.2.1.3 Image Analysis

The twenty back scattered electron images, obtained for each of the six paper samples, top and bottom, totaling 240 images in all, were subjected to image analysis using XL-Pro Image Analysis software at CSIRO, Forestry and Forest Products, Clayton, Vic.

The image was analysed by using a grey level threshold set at 111 out of a maximum of 255, which separated the filler particles adequately from the fibre particles and ensured that fibre particles were not included in the filler count.

An example of a back scattered image is shown in Figure 3.20.

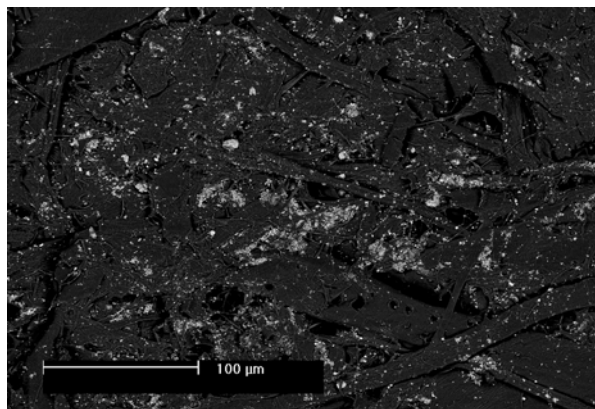


Figure 3.20 – 250X Back Scattered electron image of B2 Top side

The filler particles can then be clearly distinguished from the fibre and may be counted and allocated into nominated bins.

The bins chosen for this study are given in Table 3.6

ID Class	Size (um ²)	Colour
1	0 – 4	Red
2	4 – 8	Green
3	8 – 16	Dark Blue
4	16 – 50	Yellow
5	>50	Light Blue

Table 3.6 – Particle bins for image analysis

Figure 3.21 shows the image shown in Figure 3.20 after thresholding and allocating the particles into different bins according to the surface area size. Each particle that has been counted has then been coloured according to the classification scheme given in Table 3.6.

Classes 1 –3 are nominally very fine particles that may be considered as dust. Classes 4 –5 are more likely to be candidates for linting that may be visually seen in a printed sheet of newsprint.

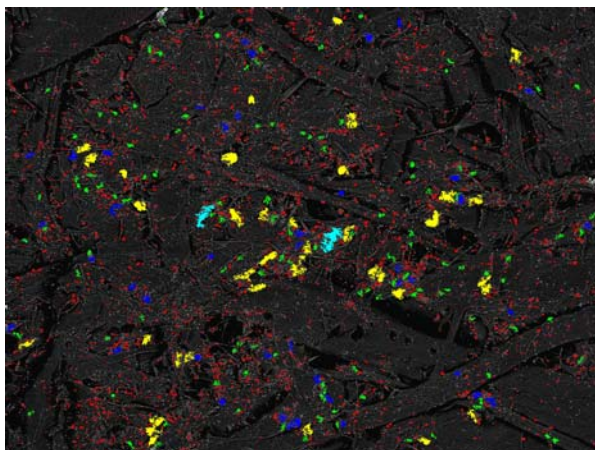


Figure 3.21 – 250X Back Scattered electron image with particles counted and binned of B2 Top side

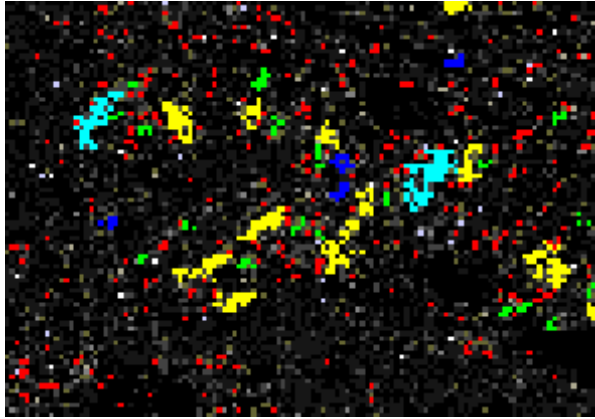


Figure 3.22 – Enlargement of detail of Figure 3.21 to illustrate more clearly relative sizes of the binned particles.

It is of utmost importance to choose the correct SEM settings to capture correct images with the SEM. If sub-optimal variables are set, then the probability of counting non filler particles as filler, or not counting all of the filler particles is increased.

Figures 3.23 and 3.24 show images that have been captured using sub-optimal conditions and subsequently when the filler has been counted with image analysis, fibre areas are counted as filler particles, as circled in Region 1 in Figure 3.24.

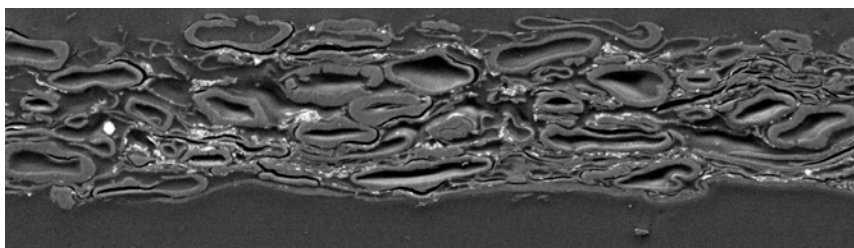


Figure 3.23 – Cross-section of newsprint taken by R. Koehly (2003), [10]

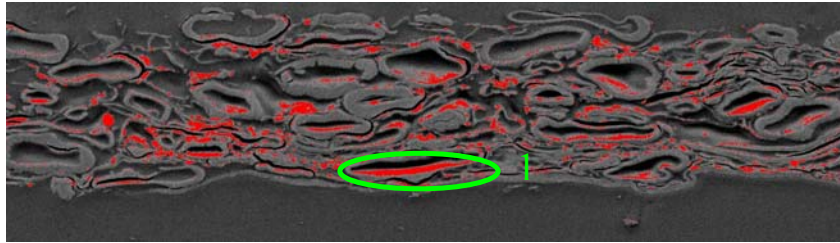


Figure 3.24 – Cross-section of newsprint taken by R. Koehly (2003) , [10] with “filler” particles incorrectly counted.

An improved set of SEM settings in Figures 3.25 and 3.26 shows Region 1, which is “light coloured” in the image, but still not counted as filler, because the thresholds have been correctly set up. The settings used were as given in Table 3.5.

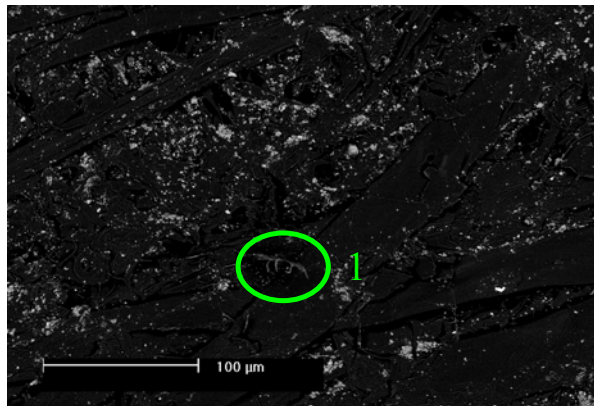


Figure 3.25 250X Back Scattered electron image of B1 Top side

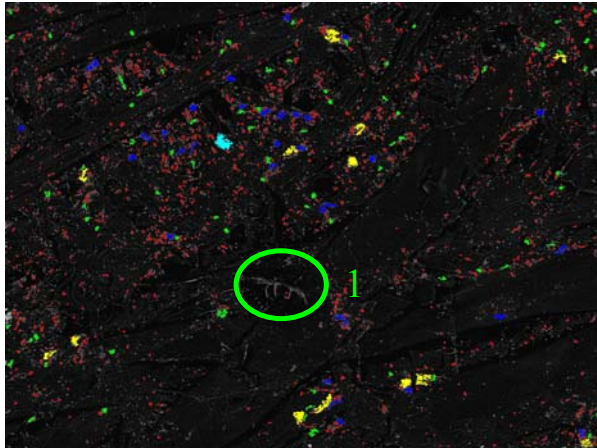


Figure 3.26 - 250X Back Scattered electron image with particles counted and binned of B1
Top side

The software (XL-Pro) has been set up to count and bin particles based on grey levels, This excludes those particles which touch the border of the image as the extension of the particle size beyond the image border is not known. This is shown clearly in Figure 3.27 where a large particle of filler has not been counted because it is adjacent to the border of the image.

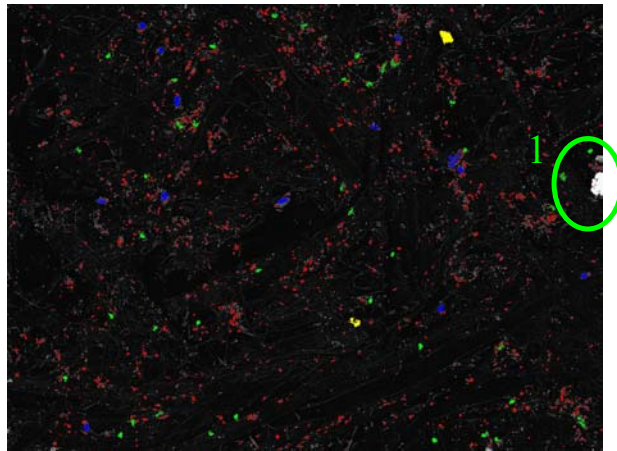


Figure 3.27 - 250X Back Scattered electron image with particles counted and binned of B2
Bottom side

The results for number and area of particles counted for each sample were tabulated and are presented in Appendix G. Each value is the average of twenty individual analyses.

3.2.2 SE Microprobe with X-Ray Detection

As the experiment set using X-Ray mapping with the energy dispersive SEM was unsuccessful as discussed in Section 3.2.1.2, a different approach was attempted. A Jeol scanning electron microprobe with a wavelength dispersive spectrometer located at CSIRO, Department of Minerals, Clayton, Vic. was used for the microscopic analysis.

A microprobe is an electron column designed to deliver stable beam currents of high intensity. These higher beam currents are used to produce sufficient characteristic x-ray intensities, analysed by a wavelength dispersive spectrometer to provide quantitative elemental analysis. [21]

Where the energy dispersive spectrometer (EDS) is useful in obtaining rapid analysis of an unknown sample, the wavelength dispersive spectrometer is preferred for obtaining quantitative information and analysis of light or trace elements.[22] Table 3.7 shows a list of advantages of both systems.

Advantages of Energy Dispersive Spectroscopy

- Compact, low cost
- Rapid
- Simultaneous multi element analysis

- High collection efficiency
- Low sensitivity to geometric effects

Advantages of Wavelength Dispersive Spectroscopy

- Higher resolution
- Higher Count rate
- Highly quantitative
- More distinct peaks
- Higher sensitivity

Table 3.7 Comparison of EDS and WDS [22]

3.2.2.1 Sample Preparation

It was chosen to prepare the samples as thin sections, since the interaction volume of x-rays is very large as shown in Figure 3.12 earlier. Preparing the samples as thin sections reduced the available interaction volume. It was recommended by CSIRO, Department of Minerals, that analysis could not be performed on bulk surface samples.

Paper samples were embedded into an epoxy resin at Monash University, School of Physics and Materials Engineering. This embedding took 4 hours to complete and an additional 2.5 hours to cure at 60⁰C.

The samples were then turned on their sides and thin sections cut from the mould containing the paper sample in the epoxy resin. The thin sections were 120 nm or 0.12 µm deep. The sectioning / cutting was performed with a diamond tipped knife of 0.2 nm in radius in an

ultra-microtome and took 8 hours to complete per sample. This is a highly specialised task and requires a high degree of precision. This work was performed by Sel Glanville from Monash University, School of Physics and Materials Engineering.

The silicates in the paper sample are very abrasive on the knife edge and as such glass knives are not appropriate as they will damage the sample. For this reason, a diamond tipped knife was used.

The samples were then glued to a layer of glassy carbon that is subsequently placed on a stub to be placed inside the SE Microprobe. Figure 3.28 shows a magnified view of the samples on the microscope stub. This was obtained with an optical microscope and camera attachment.



Figure 3.28 – 100X Four cross-sectioned samples of newsprint for SE Microprobe

3.2.2.2 Microscopic Analysis

The prepared samples were analysed using a Jeol Electron Microprobe at CSIRO, Department of Minerals, Clayton, Vic using a 25 kV beam and a beam current of 36 nanoamps. This compares to the low beam current of 5 kV used in the SEM experiments described in Section 3.2.1.2. Each sample was mapped which took 4 – 6 hours per image, depending on the step size and number of pixels. The area imaged is shaded in dark blue on Figure 3.29, as the microprobe energy is high and permanently marks the scanned area.

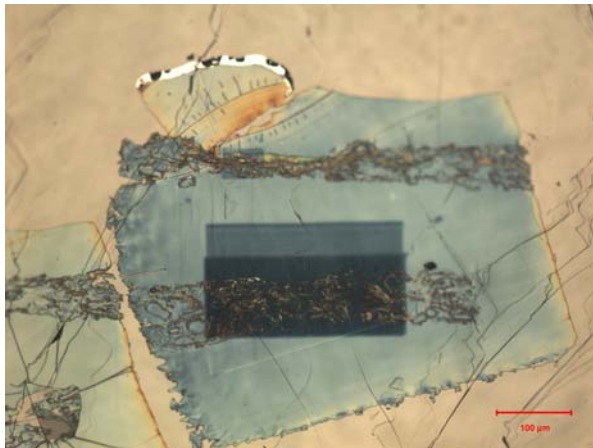


Figure 3.29 – 200X Cross-sectioned sample of B3 newsprint for SE Microprobe

Figures 3.30 and 3.31 show backscatter images taken on Sample B3. Note the rippled effect on the back scatter image due to the creasing of the glassy carbon that has been used as a support in the sample mount. The backscattered images are not as well defined as those shown in Section 3.2.1.2 that were taken by the SEM.

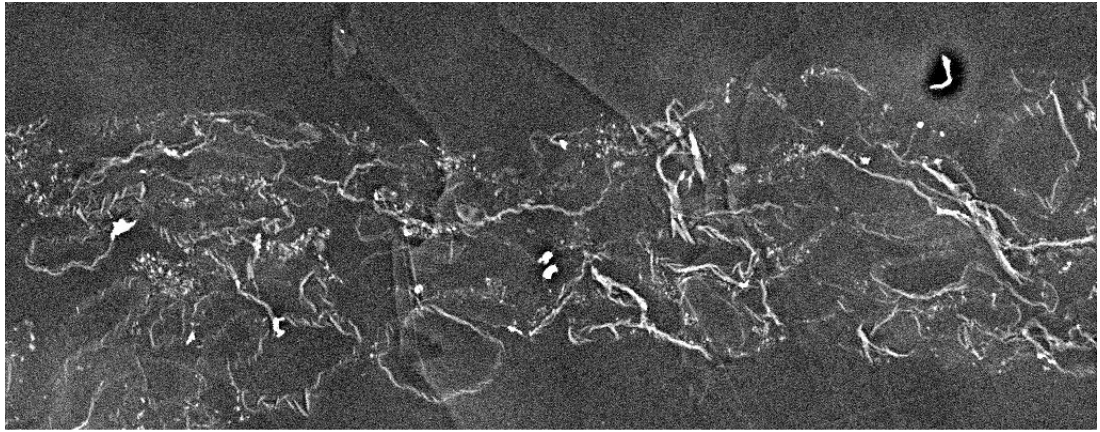


Figure 3.30 – Back scatter image of Sample B3 Cross-section

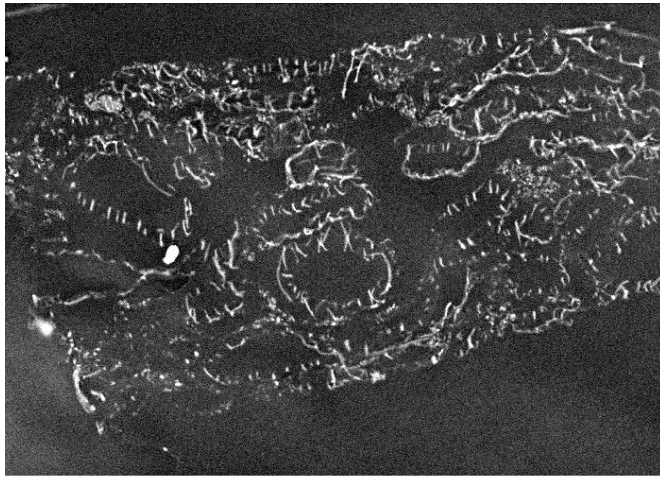


Figure 3.31 – Back scatter image of Sample B3 Cross-section

The X-Rays were detected and produced the following series of images shown in Figures 3.32 – 3.34. Trace elements such as Sodium and Iron were detected in the samples as well as the expected Silicon and Aluminium from the clay filler.

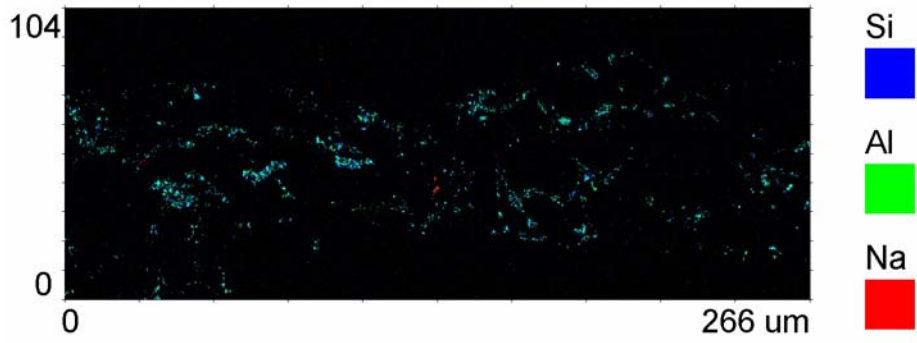


Figure 3.32 – X-Ray Map of Sample B3

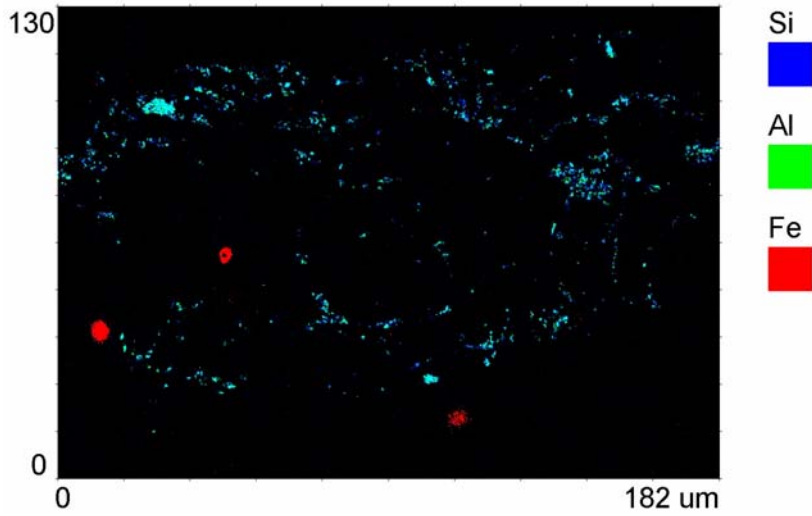


Figure 3.33 – X-Ray Map of Sample B3

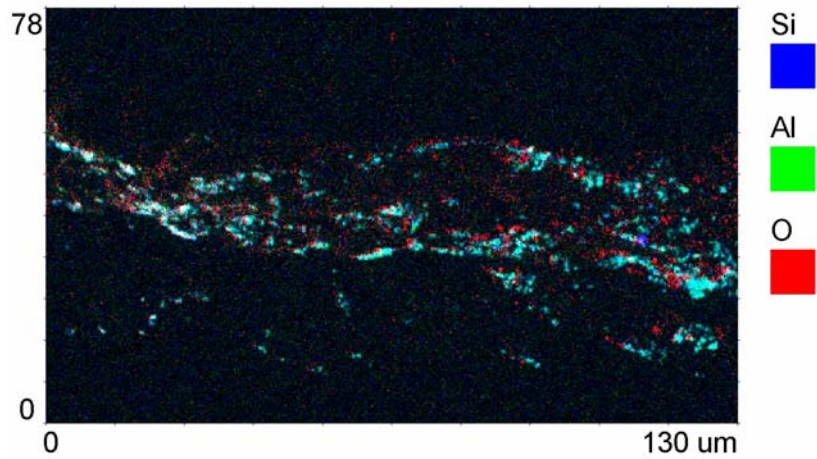


Figure 3.34 – X-Ray Map of Sample B5

Despite the higher resolution of the x-ray images with the aid of the wavelength dispersive spectrometer and the thin sections, the images obtained do not show discrete filler agglomerates. The technique does not pick up all of the elements in all locations. The images obtained can not be used to perform accurate image analysis, to determine particle size distribution.

3.2.3 X-Ray Tomography with Phase Contrast

The X-Ray ultramicroscope is a variation on the SEM principle discussed in Section 3.2.1.2. An X-Ray ultramicroscope located at CSIRO, Manufacturing & Infrastructure Technology, Clayton and operated by X-Ray Technologies (XRT) was used for this set of experiments. The X-Ray ultramicroscope is hosted within a standard SEM. The internal chamber of the SEM with the X-Ray ultramicroscope is shown in Figure 3.35

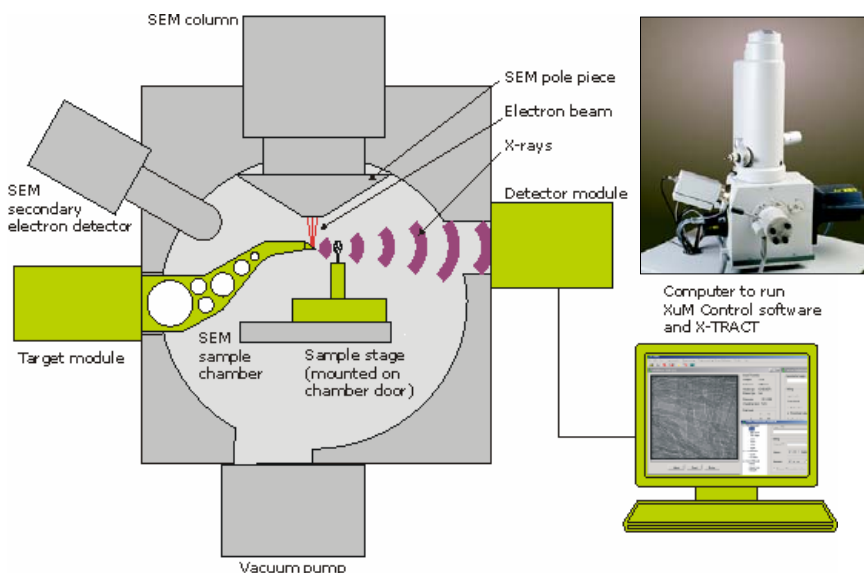


Figure 3.35 - X-Ray ultramicroscope setup. [23]

The electron beam, instead of being directed at the sample, is directed at a platinum target that generates x-Rays of approximately 8 keV. The sample (in this case, measuring 0.5 x 1 mm) is placed upright in a vice, a distance R_1 away from the x-ray source. The x-Rays travel through the sample thickness. Images are projected onto the detector, a distance R_2 away from the sample. Changing the ratio of $R_1 : R_2$ changes the magnification and also the phase contrast. This is shown in Figure 3.36.

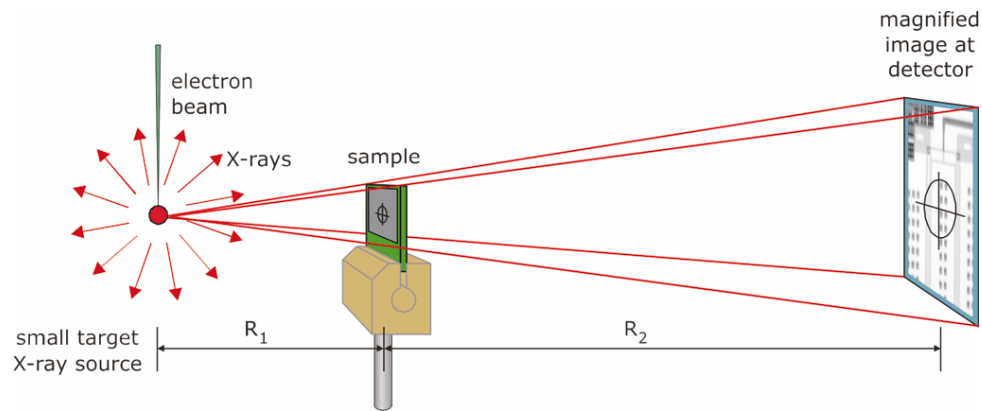


Figure 3.36 – Projection x-Ray Microscopy schematic [24]

Absorption contrast is used to create conventional x-ray images as in medical x-ray imaging. X-rays absorbed by the sample create a shadow at the detector.[24]

Phase contrast is based on the wave properties of x-rays and is a result of the refraction (not absorption) of x-rays. The effects of refracted x-rays are most notable at edges, voids or boundaries of the sample, creating an image of bright and dark fringes at the detector. The projection geometry allows the disturbed wave front to be captured.[24]

X-rays act constructively and destructively in the distance R_2 to produce the image at the detector. The image is a result of x-rays passed through the entire thickness of the stationary

sample and is thus an accumulated effect. Figure 3.37 shows the planar image of a sample of newsprint collected at the detector, spaced R_2 away from the sample. The fibre network can be seen in the image and the areas in Region 1 may be the evidence of filler.

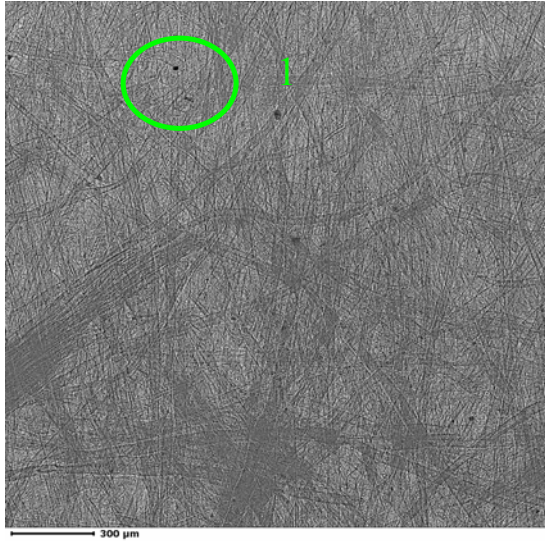


Figure 3.37 – Raw data of planar image, collected at R_2 away from sample [23]

An algorithm is then used to calculate what the image would look like at the object plane (ie $R_2 = 0$). This is shown in Figure 3.38

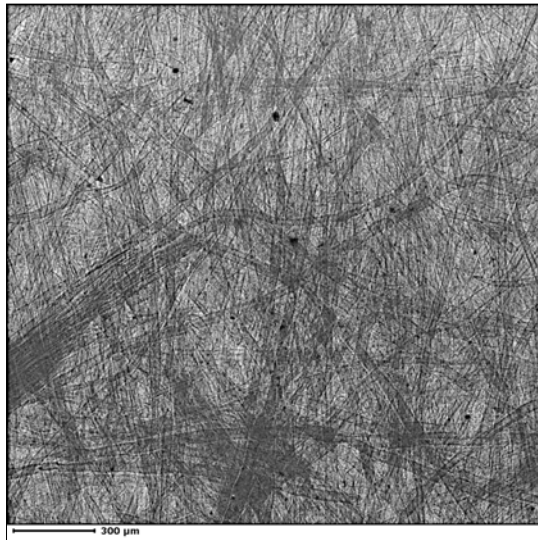


Figure 3.38 – Phase retrieved data of planar image. [23]

In the phase retrieved image, the clarity of the image is improved and further analysis can be conducted to identify particulates and construction of the sample.

Figures 3.39 and 3.40 show an area of interest. This area possibly contains fibres that have lifted out of the surface of the paper. Since the phase contrast relies on refraction, a fibre which has lifted can be seen because the refractive index for a fibre / air interface is different than for a fibre / fibre interface. These lifted fibres could theoretically be used to predict the linting propensity of the paper.

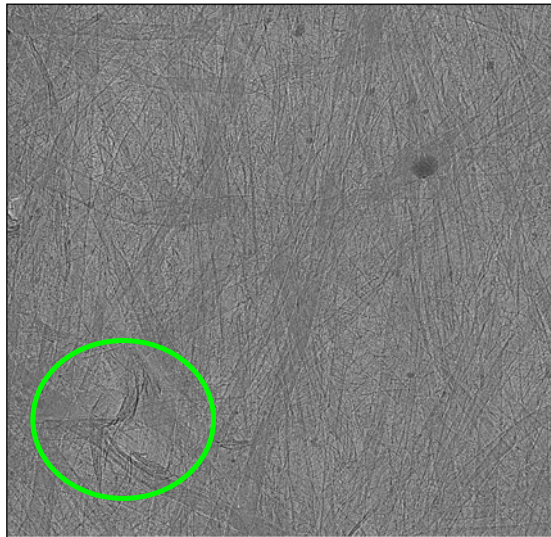


Figure 3.39 Raw Image [23]

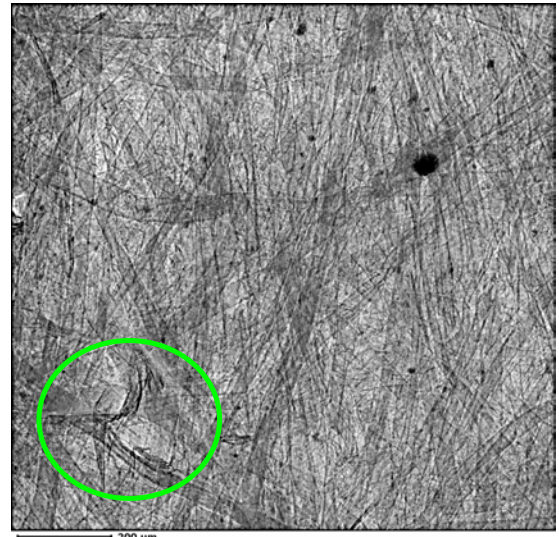


Figure 3.40 Phase retrieved image [23]

This idea is tested further by imaging an area of the paper with a tear in it. The torn area of the paper has fibres that have lifted out of the surface of the paper. Figures 3.41 and 3.42 with the torn area of paper show a similar image to that in 3.39 and 3.40 respectively.

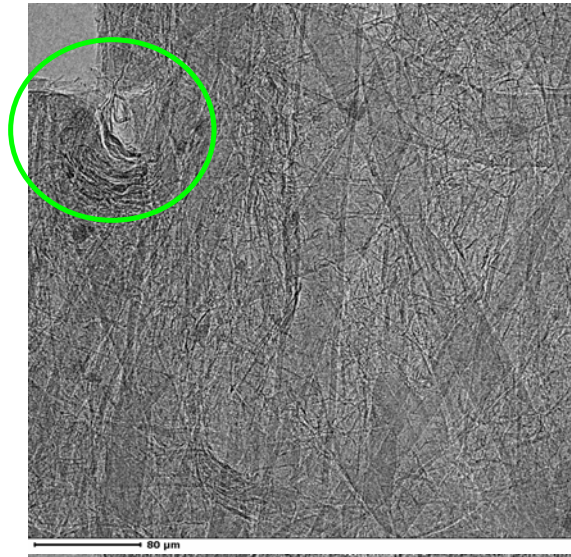


Figure 3.41 Raw Image [23]

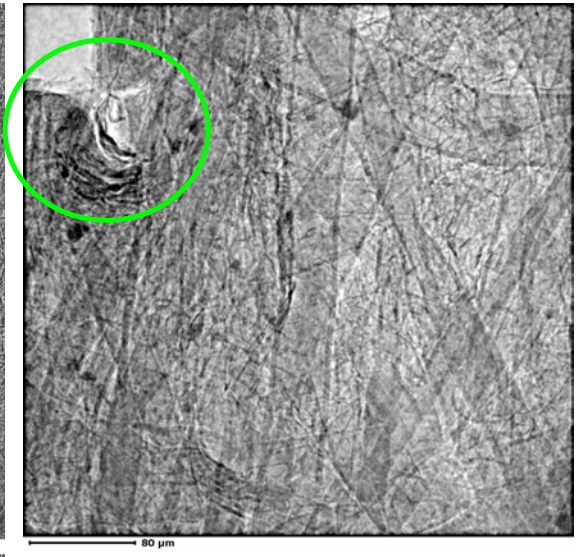


Figure 3.42 Phase retrieved image [23]

If the sample is rotated in the chamber, information can be gathered in sections / layers, enabling an entire 3D model of the sample to be reconstructed. 400 images were acquired for the 3-D reconstruction. Each image took 60 seconds to acquire and this acquisition was automated to run over-night. The 400 images are then used to construct the 3-D reconstruction that takes a further 2 hours to process. A schematic of the process is shown in Figure 3.43

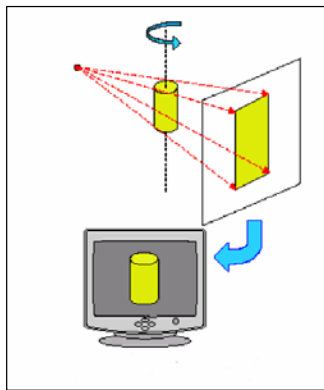


Figure 3.43 – Tomographic Reconstruction [23]

Figures 3.44 – 3.46 show the rotational views of the paper sample as it is being imaged for the 3-D reconstruction

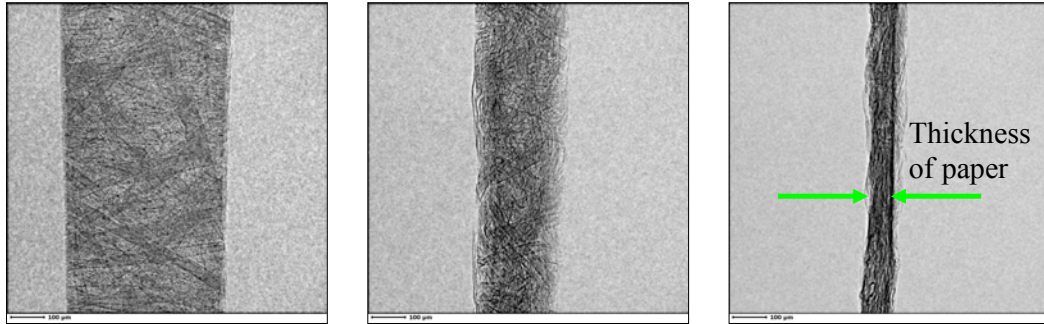


Figure 3.44 Planar View [23] Figure 3.45 Oblique View [23] Figure 3.46 side on view [23]

Figure 3.47 shows the isosurface reconstruction that is constructed by defining the surface boundary of the sample by intensity thresholding. It is constructed from the tomographic reconstruction of the X-Ray data.

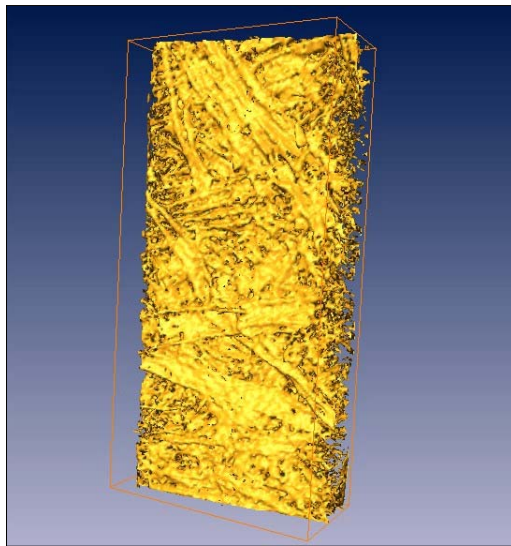


Figure 3.47 – Isosurface reconstruction of paper sample [23]

At this point, slices can be taken at any angle and at any position in the sample. Planar slices have been taken in Figures 3.48 and 3.49. An orthogonal slice has been taken in Figure 3.50.



Figure 3.48 – Virtual planar slice [23]

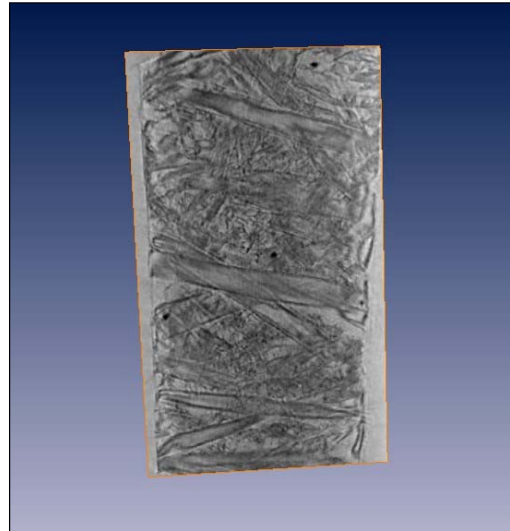


Figure 3.49 – Virtual planar slice [23]

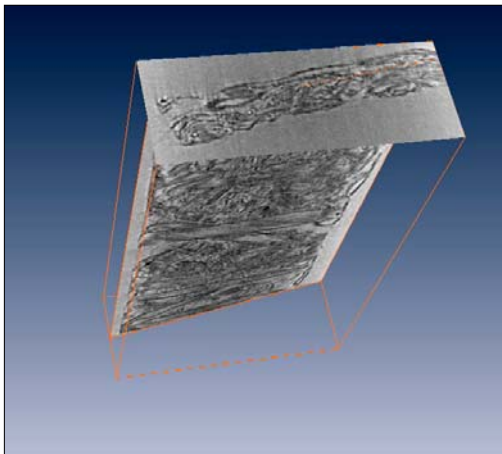


Figure 3.50 – Orthogonal slicing of paper sample [23]

It is possible to select particles based on density and segment them from the rest of the sample. This is the process by which filler particles could possibly be selected and

segmented from the fibre network. Figure 3.51 shows the segmentation of the dark particles that are believed to be filler. Slices could then be taken in any direction in the volume to determine filler distribution.



Figure 3.51 – Particulates in sample volume.[23]

This method has been investigated as a proof of concept at this stage. The author recommends that this method be investigated further to determine the usefulness in determining filler size distributions in paper samples.

Extended work is required in selecting the appropriate intensity thresholds to separate the filler particles from the fibre network. The resolution is $0.3\ \mu\text{m}$ and limited sample preparation is required. This is a non-destructive test method. Sample slices can be taken with thickness of $1\text{-}2\ \mu\text{m}$. The slice thickness is a function of the resolution of the original images that make up the 3-D reconstruction .

3.2.4 FTIR Spectroscopy

Fourier Transform Infrared (FTIR) Spectroscopy is an analytical technique used to identify materials in a sample. A light source is used to produce light in the infrared (IR) region and the sample is subjected to IR light. The sample absorbs different IR light wavelengths according to its chemical properties (molecular components and bonds). A detector is used to collect the radiation that passes through the sample and a mathematical function known as a fourier transform is used to produce a spectrum.

3.2.4.1 Determination of spectra

The Bruker – Equinox 55 FTIR Spectrometer, Department of Chemistry, Monash University was used to obtain spectral data for cellulose and filler.

Two samples of cellulose (fibrous long and microgranular) and one sample of clay filler were analysed. A small amount of sample was placed onto a diamond plate and pressure applied via an anvil to ensure that the sample was flat. The infrared radiation penetrates 2 μm into the sample, measuring the spectra with FTIR in reflectance mode, using a diamond ATR plate. The sample area is 1 mm in diameter.

Figures 3.52 and 3.53 show the spectra obtained for the cellulose fibrous long and cellulose microgranular respectively.

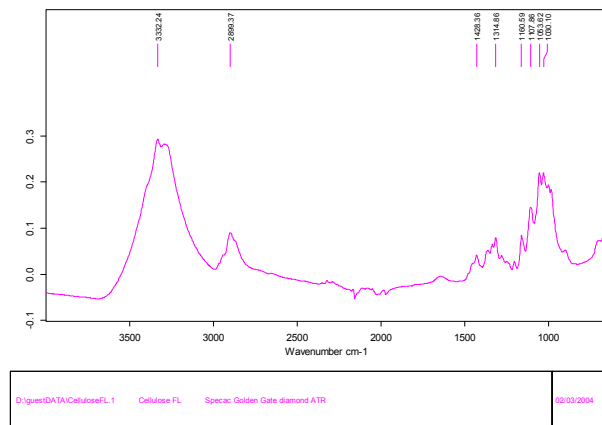


Figure 3.52 – Spectrum of cellulose fibrous long

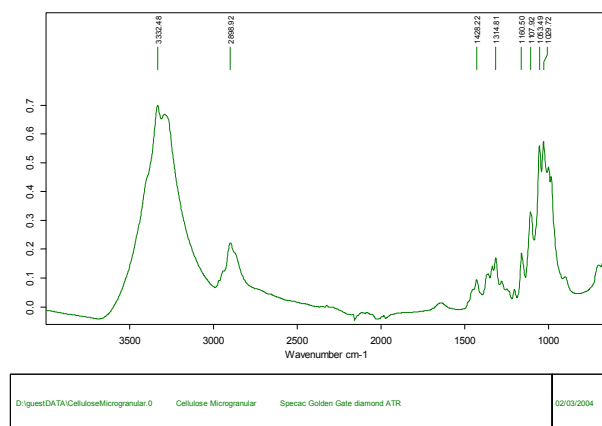


Figure 3.53 – Spectrum of cellulose microgranular

As expected the two spectra for different samples of cellulose are essentially the same. The first peak at 3332 is due to the –OH bond. The second peak at 2899 is due to the –CH₃ and –CH₂CH₃ groups. The large group of peaks from 1428 – 1030 are due to other organic bonds and intra-molecular interactions in the cellulose. These bonds and chemical groups can be seen in Figure 3.54. The chemical formula for cellulose is (C₆H₁₀O₅)ⁿ where n is the degree of polymerisation.[25]

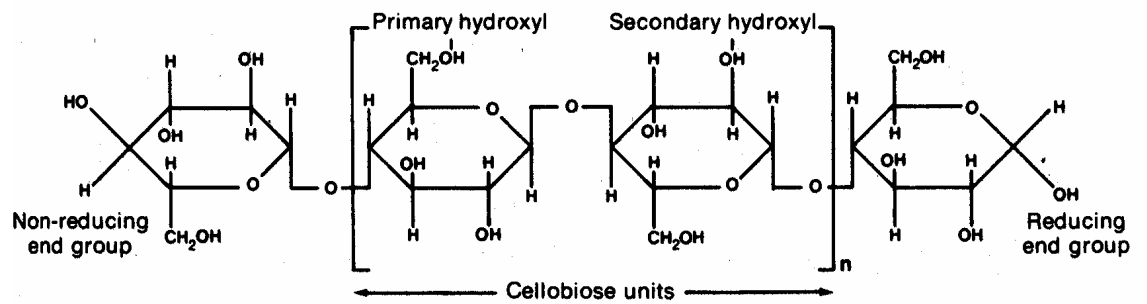


Figure 3.54 – Chemical structure of cellulose [25]

When analyzing a paper structure, other components attached to the cellulose must also be considered, such as lignin, found in newsprint. Figure 3.55 shows the chemical structure of lignin and the associated phenyl propane units.[25] Depending on the pulping used to process the wood fibres, different modifications to the base components would occur, resulting in different spectra.

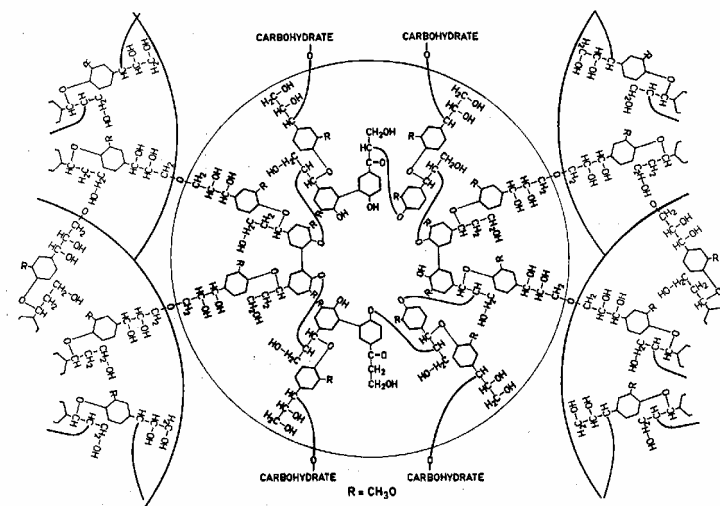


Figure 3.55 – Chemical structure of lignin [25]

The spectra for lignin is shown in Figure 3.56. There are no prominent peaks and will not interfere with the distinction between fibre and filler. The parabolic shape of the curve is due to the white kraft liquor in which the lignin is dissolved. The actual peaks from the lignin are individually marked.

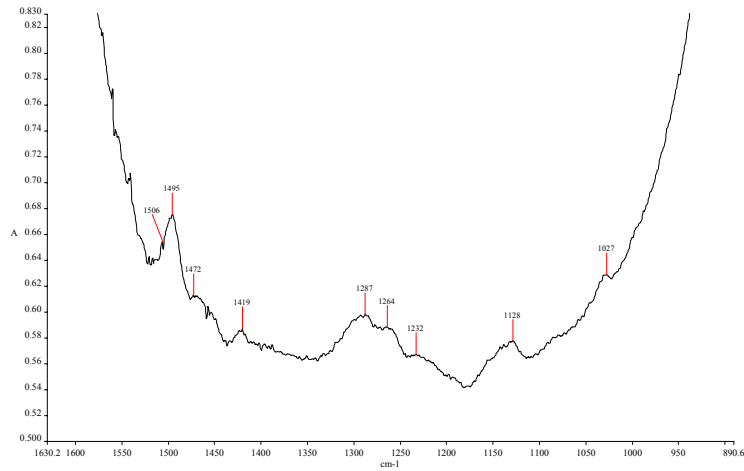


Figure 3.56 – Spectrum for lignin.[26]

The clay was analysed by Bruker FTIR and the spectra is shown in Figure 3.57.

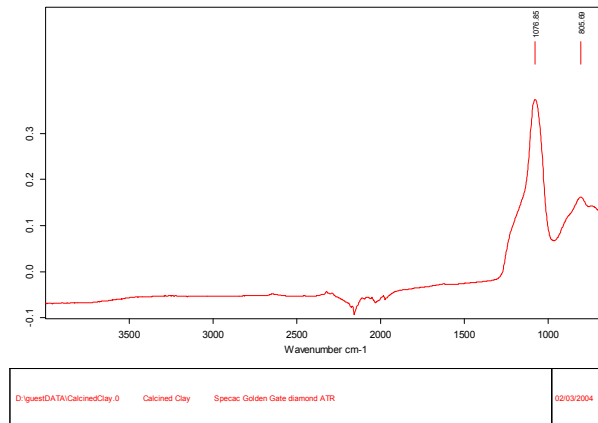


Figure 3.57 – Spectrum for calcined clay

The chemical formula for calcined clay is $\text{Al}_2\text{Si}_2\text{O}_7$. [27] The major peak at 1077 is due to the Al-O and Si-O bonds. These overlap as they emit spectra at similar wave numbers.

The small dip in the spectra around 2200 is due to the diamond plate used in the measurement. This small dip can be found in all of the spectra and should be ignored.

3.2.4.2 Paper measurement

Knowing the spectra for the major individual components of the newsprint, a prediction of the spectra obtained for a piece of newsprint can be made. It will be a combination of both cellulose and clay spectra, shown in Figure 3.58.

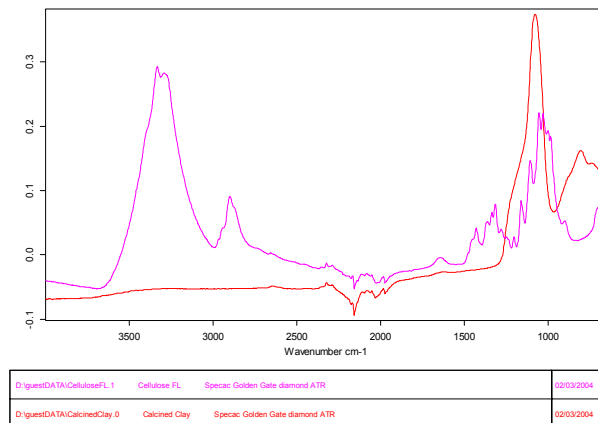


Figure 3.58 – Spectra of Clay and cellulose overlaid.

The cellulose spectra can be subtracted from the spectra of the paper sample to give the filler sample only. The paper sample can then be mapped using reflectance on the FTIR microscope attachment to provide a map of filler distribution across the surface of the paper.

This in turn could be analysed using image analysis software to quantify the particle size distribution of the filler in the paper surface.

FTIR Microspectroscopy equipment is available in APPI, Department of Chemical Engineering, Monash University. The equipment was purchased recently and is currently undergoing commissioning. It was thought that this would be a useful tool to map filler distribution as it has a resolution of 6 μm and the spectra of the fibre and filler should be separable. However this equipment was not available due to problems in commissioning.

This technique has been investigated as a proof of concept and the author recommends that further work be conducted with the FTIR to investigate the method. The infrared beam from the FTIR is focused onto a sample placed in the microscope attachment. The requirements for sample preparation are simple and the sensitivity of detection is high.[28]

4.0 RESULTS AND DISCUSSION

In order to compare the material removed in the laboratory printing experiments with the filler size distributions measured in the surface of the paper, correlations between the following properties were investigated.

- A. Fine / Filler lint area from IGT test print (Class 0 – 0.05 mm²).
- B. Fibre lint area from IGT test print (Class 0.1 – 10 mm²)
- C. Total Lint area from IGT test print (mm²)
- D. Total Filler Area from SEM, including border particles (µm²)
- E. Percentage of SEM image covered by Filler (%)
- F. Filler Area from SEM > 50 µm²
- G. Filler Area from SEM > 16 µm²
- H. Filler Area from SEM > 8 µm²
- I. Total Filler Area from SEM, excluding border particles (µm²)
- J. Treeline Result
- K. Heidelberg Test lint (gsm)

The full data sets for the properties are given as follows :

A-C : Appendix E

D – I : Appendix G

J- K : Appendix I

The treeline result is an indication of the presence of filler vs fines in the lint as discussed in Section 3.1.3. Figure 4.1 shows that the amount of filler deposited on the Heidelberg press blanket in the tree line area is generally proportional to the amount of filler / fines removed in the IGT test print.

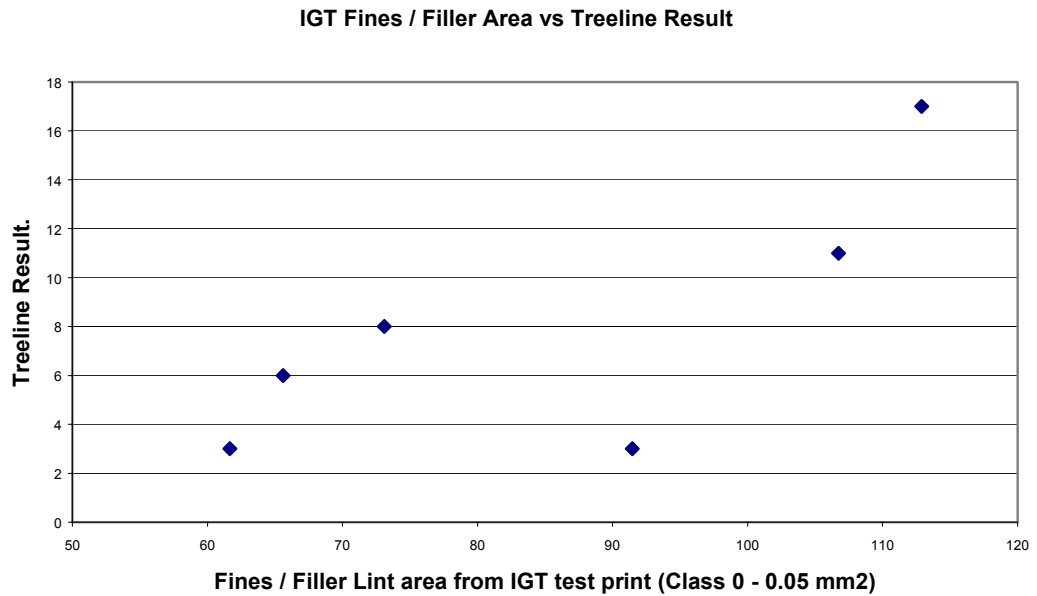


Figure 4.1 - IGT Fines / Filler Area vs Treeline Result

Figure 4.2 shows that the amount of filler deposited on the Heidelberg press blanket in the treeline area is also generally proportional to the total lint area removed in the IGT test print as the total area removed in the IGT test print is dominated by the fines / filler area.

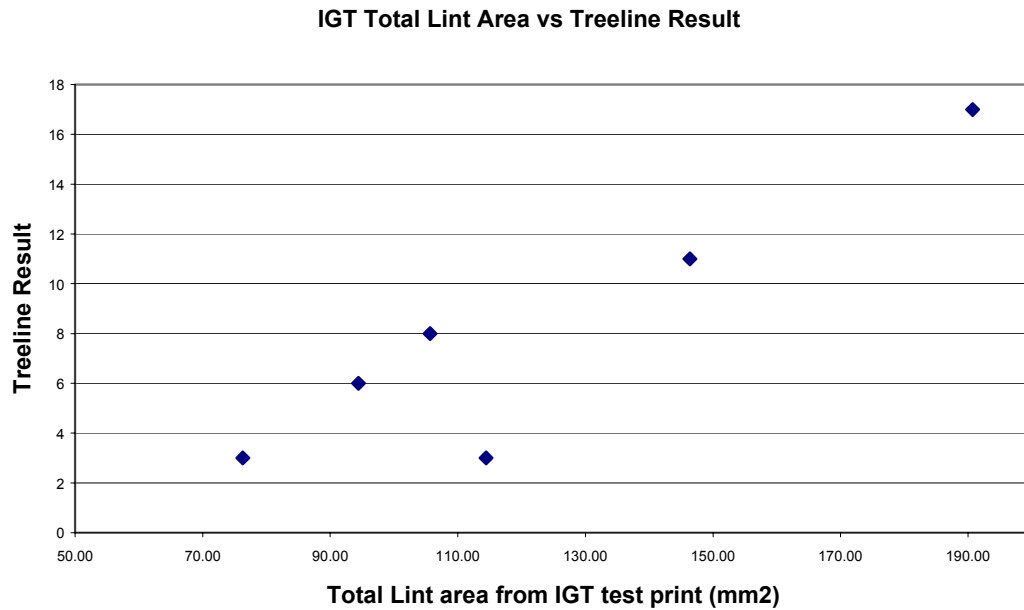


Figure 4.2 - IGT Total Lint Area vs Treeline Result

The Heidelberg tests and the IGT series of experiments has shown a good correlation between the amount of filler deposited on the Heidelberg Offset press and the amount of fines and filler removed by the IGT test print. A more robust correlation may be possible with more data. The Treeline data is limited to the bottom side of the sheet and hence the data is limited. The full data for the Treeline may be found in Appendix I.

No correlation could be found between the overall Heidelberg lint count and the amount of lint removed in the IGT test prints. This may be due to a variety of factors including differences in ink, printing pressure, printing speed and the small range of Heidelberg values from 5.5 to 7.5.

No correlation could be found between the amount of lint removed in the IGT test print and the amount of filler detected in the surface of the sheet by SEM, as is shown in Figure 4.3. There is a distinct outlier in the data set. The experiments were repeated for this outlier (B3 bottom) to confirm the results, which remained unchanged from the original set of experiments. Sample B3 bottom had a very high propensity for lint, as measured by the IGT and a very high percentage of filler in the sheet surface (5.52%) compared to other samples that had percentages as low as 1.2 %.

Similarly, there was no correlation between the amount of lint removed in the IGT test print and the amount of filler detected in the surface of the sheet by SEM from either $>50 \mu\text{m}^2$, $>16 \mu\text{m}^2$ or $>8 \mu\text{m}^2$ particle size ranges. The B3 bottom sample, remains an obvious outlier.

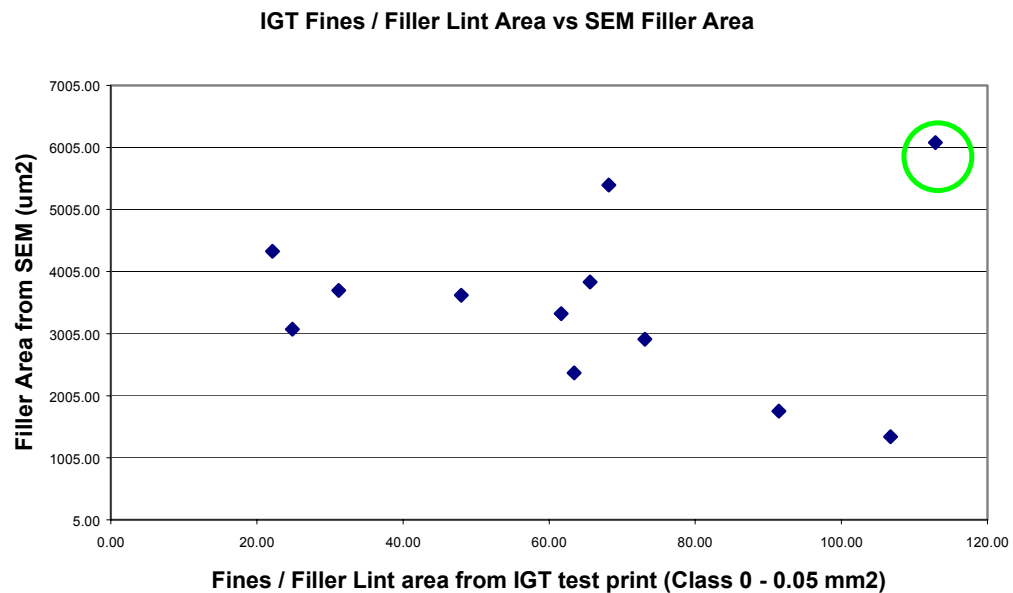


Figure 4.3 - IGT Fines / Filler Area vs Filler area from SEM

There is a fair correlation between the amount of filler detected in the surface of the sheet by SEM and the Treeline result as shown in Figure 4.4. The greater the amount of filler found in the surface of the sheet, the higher the lint count of the Treeline result which is related to the amount of filler lint particles found on the test print of the Heidelberg test. Substantially more Treeline data would prove this correlation either way.

The correlation could possibly be improved if the Heidelberg data, main and treeline, were further separated to determine the filler and fibre content of each. The treeline data, although predominantly related to filler content, would also have a fibrous content.

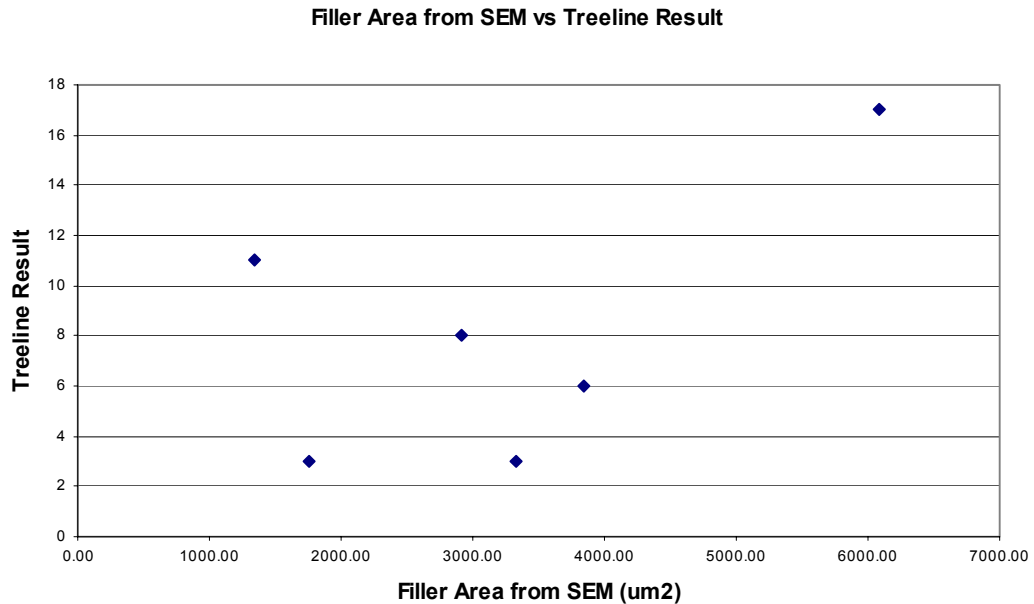


Figure 4.4 - Filler area from SEM vs Treeline result

No correlation could be found between the Heidelberg lint count and the amount of filler detected in the surface of the sheet by SEM. This may be due to a variety of factors

including ink, printing pressure, printing speed and the small range of Heidelberg values from 5.5 to 7.5.

Similarly, there was no correlation between the Heidelberg lint count and the amount of filler detected in the surface of the sheet by SEM from either $>50 \mu\text{m}^2$, $> 16 \mu\text{m}^2$ or $>8 \mu\text{m}^2$ particle size ranges.

The samples of paper given in Table 3.4 were all samples of the same grade of paper (Image / Norstar) manufactured at Norske Skog Boyer Mill. The paper is made with the same furnish ratios and filler content. Despite this, the amount of filler found in the surface of the sheet by SEM back scatter and image analysis varies considerably.

The full data set is given in Appendix G. As an example, sample B3 Top contained on average $4413.60 \mu\text{m}^2$ of filler in the surface of the sheet (4 %), whereas Sample B6 Top contained $1738.88 \mu\text{m}^2$ of filler in the surface of the sheet (1.6%). These differences show that the content of filler at the surface of the paper differs considerably despite aims to make the paper consistently.

Figures 4.5 and 4.6 show an example of the back scatter images of B3 top and B6 top respectively, showing the contrast in filler area and percentage.

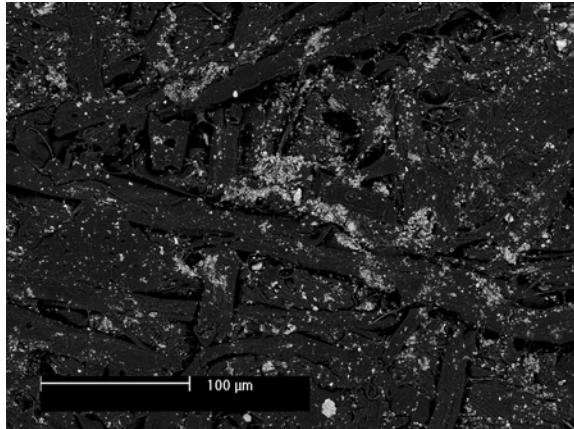


Figure 4.5 – 250 X Back Scattered Electron image of B3 top side (higher filler content)

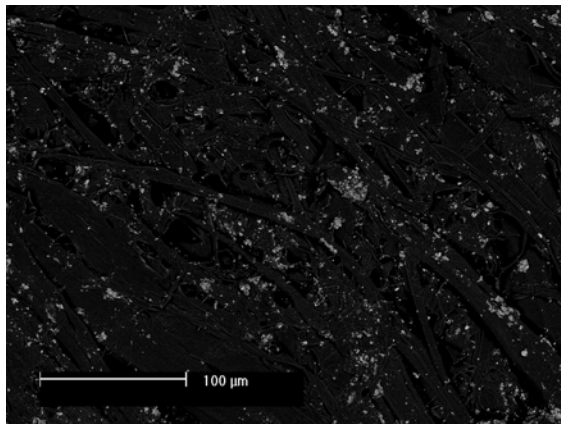


Figure 4.6 – 250 X Back Scattered Electron image of B6 top side (lower filler content)

Figure 4.7 shows the difference in filler percentage as measured by SEM back scatter in the top and bottom surfaces of the paper samples given in Table 3.4.

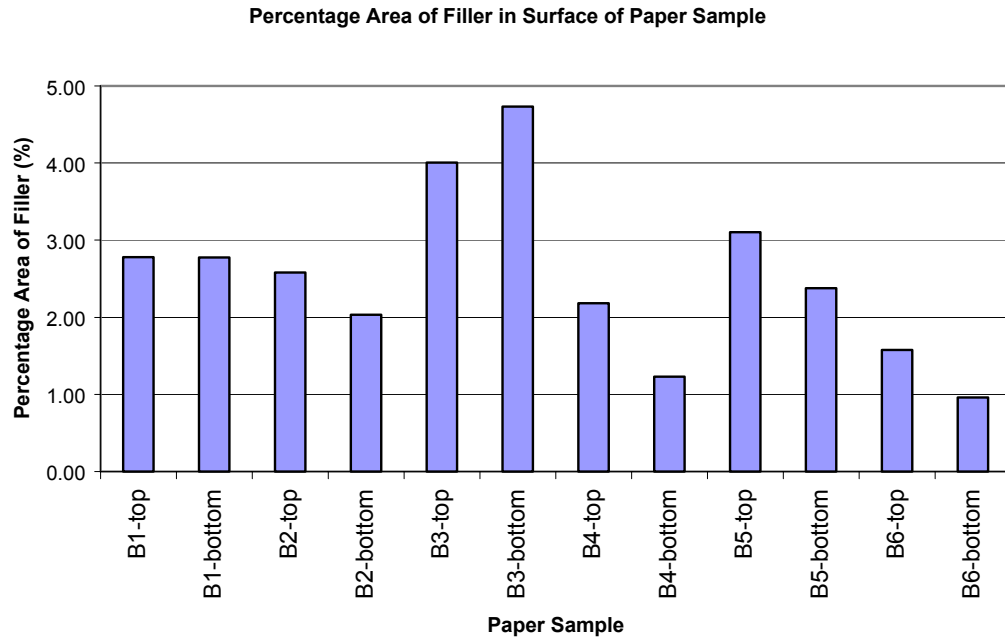


Figure 4.7 - Percentage Area of Filler in surface of Paper sample

Figure 4.8 shows the difference in % of large ($> 8 \mu\text{m}^2$) agglomerates of filler as measured by SEM back scatter in the top and bottom surfaces of the paper samples given in Table 3.4.

It can be concluded that there are substantial differences in the filler particle size distribution in the series of paper samples given in Table 3.4

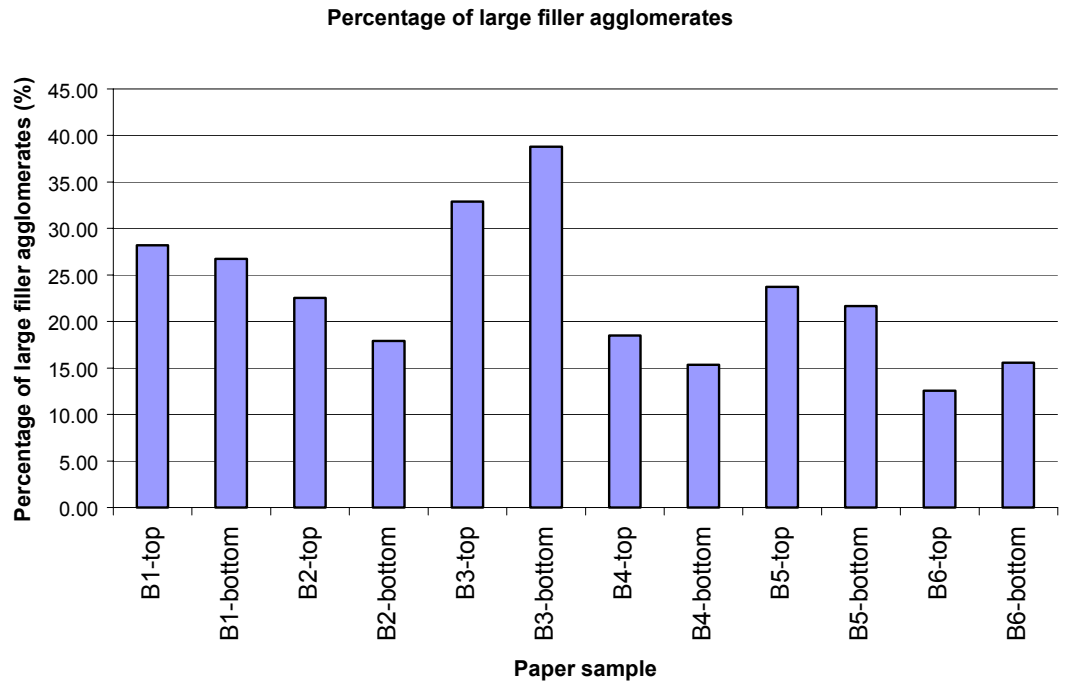


Figure 4.8 - Percentage of Large ($> 8 \mu\text{m}^2$) Agglomerates of Total Filler Area

5.0 CONCLUSIONS

The IGT Printability tester is an appropriate laboratory scale printing test unit to artificially remove filler from sheets of newsprint / paper. The IGT Printability tester provides repeatable results when evaluating the linting propensity of a series of papers, if run under the same set of experiment variables. It is difficult to quantify and qualify whether the source of lint has been from filler or small fibre fragments / fines. It is difficult to distinguish between print mottle effects, non homogenous paper surface properties and lint from filler / fines / fibre fragments.

Scanning electron microscopy coupled with backscatter detection offers an efficient method of imaging the surface of the sheet with good distinction between fibrous and filler components.

X-Ray detection in the SEM does not supply images of suitable quality to calculate the size distribution of the filler agglomerates. It does however detect the elemental constitution of a sample. Scanning electron microprobe with X-Ray detection does not supply images of suitable quality where the filler size distribution of the filler agglomerates can be calculated. It does however also detect elemental constitution of a sample.

X-Ray Tomography with Phase contrast has been evaluated as a proof of concept and shows good promise as a suitable method for the determination of filler distribution through a paper sample. Further experimental work is required to produce a proven method.

The spectra of filler and fibre as measured by FTIR are sufficiently different to enable excellent separation of signal / spectra. A scanning FTIR could potentially be used to map filler distribution on the surface of paper.

The treeline figure increases with increasing amount of lint measured on the IGT test print. The treeline figure increases with increasing amount of filler measured in the surface of the sheet as measured by SEM and image analysis. There is no robust correlation between linted areas as measured in IGT test prints, filler areas as measured by SEM and image analysis or Heidelberg Lint results. The samples measured showed wide variability in filler content and distribution, despite all being the same grade of paper and with the same nominal filler content.

6.0 RECOMMENDATIONS FOR FURTHER WORK

1. Conduct IGT Printability tester experiments including the addition of water with a second printing disc. In offset printing, both fountain solution and water emulsified ink are added to the paper surface. An improved laboratory test which may replicate the lint removed in the offset printing process should include two modes of printing, one where water / fountain solution is added and then a second, where ink of a tack equivalent to emulsified offset print is added. [6]
2. Investigate ability of X-Ray Tomography with phase contrast to quantify lifted fibres from paper surface
3. Extend experimental work with X-Ray Tomography with phase contrast to threshold intensity maps to segregate filler and fibre from 3-D reconstruction of paper volume.
4. Use the FTIR to provide elemental maps of the paper surface which may in turn be analysed by image analysis for filler particles size distribution
5. Obtain more data for the Heidelberg tests, both for the treeline and overall measurement to confirm correlations with amount of lint removed in the IGT print test and amount of filler measured in surface of paper by SEM and image analysis. The Heidelberg results should be further broken down into filler and fibre content. Hopefully a better correlation can be found when the filler distribution measured in the SEM can be plotted against the filler and fibre components of the Heidelberg overall and treeline results,

6. Continue to use SEM with back scatter detection to obtain images of paper surface, which may be subjected to image analysis for quantification of filler particle size distribution.

7. Investigate whether a dye exists which can preferentially dye paper fibres and not the filler in a sheet or vice versa. This would be an efficient and quick way to quantify filler particle size distribution of the sheet.

7.0 REFERENCES

1. Mangin, P.J., A critical review of the effect of printing parameters on the linting propensity of paper, Journal of Pulp and Paper Science, Vol 17, No.5 pp 156 – 163, September 1991
2. IFRA (Association for media publishers, Damstadt, Germany) Special Report Materials 1.19, The phenomenon of linting in newsprint printing, March 2000
3. Ionides, G.N., The linting tendency of newsprint – a general review, Paperi ja Puu – Papper och Trä, No.4, pp 298 – 306, 1984
4. Wood, J.R. and Karnis, A., Linting propensity of mechanical pulps, Pulp and Paper Canada, Vol 93, No 7, pp 17 – 24, 1992
5. Papasergio, R.I., The measurement of linting tendencies of mechanical pulps, Appita Preprint, A27.1
6. Mangin, P.J. and Silvy, J. Surface pore structure, ink flow and fibre removal during printing, International Paper Physics Seminar, Kalamazoo, MI USA, 1990
7. Mangin, P.J. and Dalphond, J.E., A novel approach to evaluate the linting propensity of newsprint : Part 1:Background and Test procedure, Pulp and Paper Canada, Vol 93, No 12, pp 176 – 182, 1992
8. Heintze, H.U. and Ravary, R.E., An economical means to measure and characterize lint, Pulp and Paper Canada, Vol 95, No 6, pp 47 – 50, 1994
9. Lindem, E and Moller, K., The Dagbladet full scale printing trials – Part 3 : Linting in four colour offset printing, Tappi Journal, Vol 77, No.7, pp 185 – 191, July 1994
10. Koehly, R. Effects of Wet End Chemistry on linting of filler, Diplôme Ingénieur EFPG, France / APPI, Australia, 2003

11. Lorz, R., Baumann, P. and Schall, N. New Technologies to reduce filler separation in Offset Printing, Pira 3rd International Conference, UK, 2001
12. Wood, J.R., Imada, S.E., Beaulieu, S. and Kerr, R.B., Reduction of Offset Linting – A comparison of six mills : Part 1. Pressroom Effects, Pulp and Paper Canada, Vol 96, No. 10, pp 33 – 349, 1995
13. Moller, K. et al, Factors influencing linting in offset printing of newsprint, Proceedings of Appita Conference, 1995, pp 115 – 121
14. Collins, N.J., Rosson, A.J. and Jenkins, S., Print quality studies on a Heidelberg test press, Appita, Vol 43, No 6, pp 437 – 445, November 1990
15. Mangin, P.J. and Dalphond, J.E., A novel approach to evaluate linting propensity of newsprint : Part 2 : Case Studies, Pulp and Paper Canada, Vol 94, No 1, pp 23 – 28, 1993
16. Waech, T.G., Offset lint testing by image analysis, Pulp and Paper Canada, Vol 93, No 9, pp 60 – 65, 1992
17. Domtar Lint Tester Product Brochure, OpTest Equipment Inc, Ontario Canada
18. Williams, G.J. and Drummond, J.G., Preparation of large sections for the microscopical study of paper structure, Tappi Proceedings, 1994 Papermakers Conference, pp 517 – 523
19. Gibbon, D.L., Gray, R.T. and Simon, G.C., Stereological and Chemical analysis of paper cross-sections, Tappi Proceedings, 1998 Coating / Papermakers Conference, pp 435 – 454

20. Boulineau, J Jr. and Davis, J., Dusting Problem Investigation for Norske Skog Boyer, Part III, Technology Report 0208/1, July 2002
21. Vaughan, D (Ed), Energy Dispersive X-Ray Microanalysis – An Introduction, USA, 1989
22. Postek, M.T. et al, Scanning Electron Microscopy – A student’s handbook, Ladd Research Industries, USA, 2001
23. XRT Presentation, given by Julie Sheffield Parker, 12th March 2004
24. XRT Product Profile, The X-Ray Ultramicroscope, EDAX / XRT, USA
25. Smook, G.A., Handbook for pulp and paper technologists, Canada, 1982
26. Hoang, V., Personal Communication, APPI, Australia, 2004
27. Imerys Pigments and Additives Group, Material Safety Data Sheet, Alphatex Dry (Calcined Kaolin Clay / Anhydrous Aluminium Silicate), USA, 2004
28. Günzler, H and Gremlich, H.U., IR Spectroscopy – An Introduction, Wiley-VCH, Germany, 2002

APPENDIX A – Norske Skog Procedure for IGT Testing

Manual: NSTL PPSG Procedures	Document Number: 140-A3-06-WI	
Subject: Surface Strength of Newsprint - Picking	Page: 1 of 5	Version: 8
	Prepared By: M Howard	
Authorised By: M Howard	Date Issued: 27 February 2002	

1.0 PURPOSE

This work instruction describes the test method used for measuring the surface strength of newsprint (picking).

2.0 SCOPE

This work instruction shall apply to people carrying out laboratory print testing who have had training.

3.0 DOCUMENTS AND FORMS

Not applicable to this work instruction.

4.0 REFERENCES

- 4.1 ISO Standard 3783. Paper and Board - Determination of Resistance to Picking - Accelerating Speed Method Using the IGT Tester (electric model) - Available from the PPSG Adviser (Printability).
- 4.2 Instruction Manual IGT Inking Unit AE - Available from the PPSG Adviser (Printability).
- 4.3 Instruction Manual IGT Printability Tester AIC 2-5 - Available from the PPSG Adviser (Printability).
- 4.4 PAPRO Report No. C162, October 1988, Updated IGT Printability Test Methods at September 1988 - Available from Technical Department Files.
- * 4.5 140-A3-11-WI Use of Image Analyser for Measuring Pick Test Strips and Ink Coverage.
- 4.6 Fume Cupboard Instructions.

5.0 **DEFINITIONS**

5.1 Surface strength, picking: The rupture of the surface of newsprint and/or the removal of fibres from the surface of newsprint.

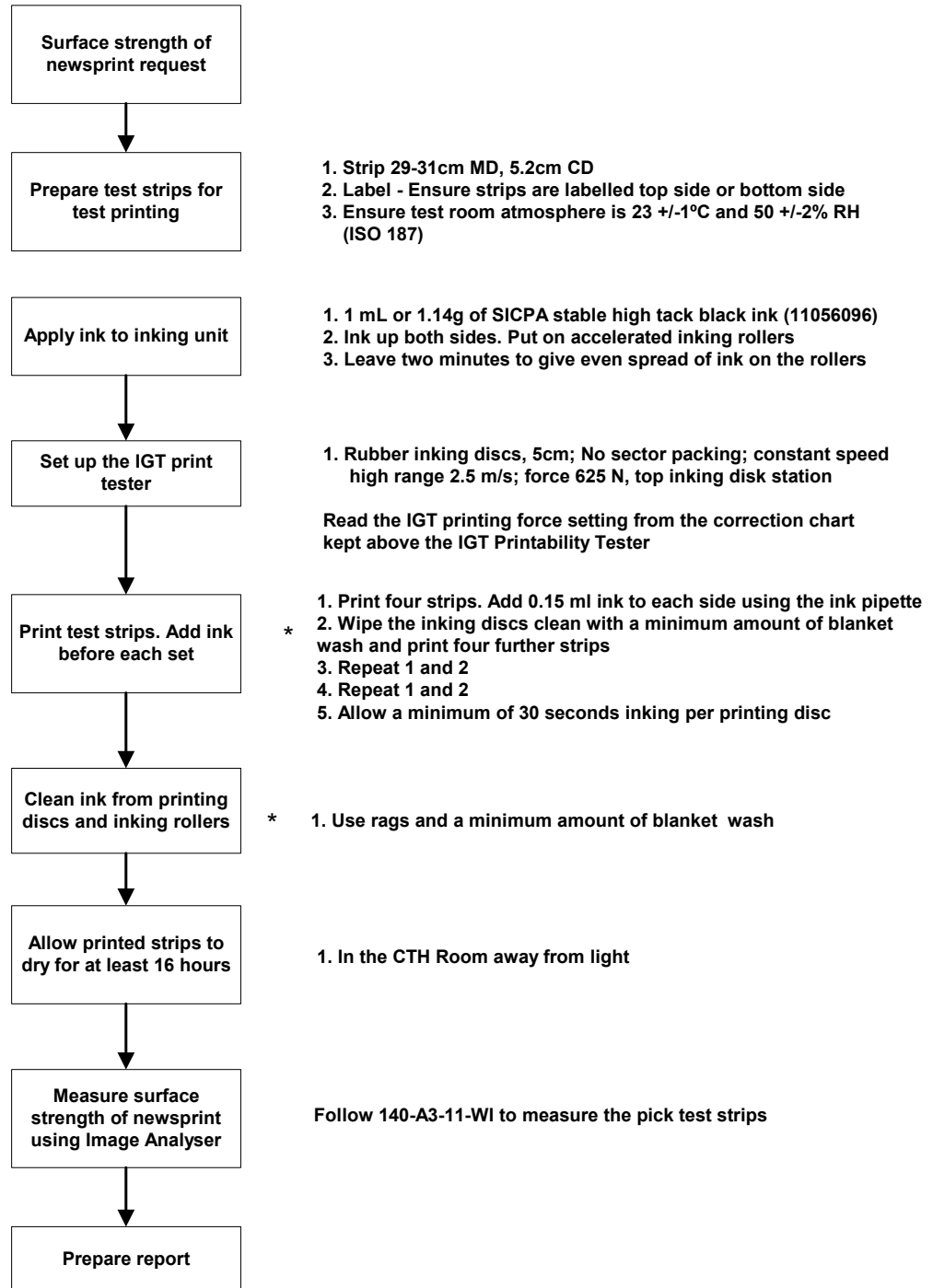
5.2 CTH Room: Constant Temperature and Humidity Room within the Technical Centre

* **5.3** Blanket Wash
remove and Chemical cleaning solution used to clean ink from the IGT print tester.

6.0 **CONTROL**

This work instruction is controlled by the PPSG Adviser (Printability).

7.0 FLOWCHART



8.0 **PROCEDURE**

8.1 **SURFACE STRENGTH OF NEWSPRINT**

To date, there has not been a satisfactory method available to measure the absolute surface strength of paper (see ISO 3783). With the IGT equipment, practical limitations restrict the number of samples in a group to four. Sometimes a so-called "standard" sample of paper is used as one of these four samples. In this way, the unknown samples can be compared against the "standard". In this fashion, a crude benchmark is established to compare between groups of four tests.

This method is based on ISO Standard 3783 and PAPRO Report No. C162. It has needed to be extensively modified to suit Tasman's needs, and now uses a constant, rather than accelerating speed.

8.2 **PREPARE TEST STRIPS FOR TEST PRINTING**

When labeling, make sure the sides of the newsprint are not interchanged. A good system is to cut four strips for each sample being tested and label them "1", "2", "3", "4" and TS or BS before starting to print.

As ink tacks are sensitive to temperature changes, it is necessary to ensure the CTH room atmosphere is within ISO specifications (temperature 23 ± 1 °C relative humidity $50 \pm 2\%$).

8.3 **APPLY INK TO INKING UNIT**

Switch on the fume cupboard and leave on until at least 10 minutes after cleaning up. The ink currently being used is SICPA stable high tack black ink (11056096). Fill the ink pipette.

Each side of the inking unit has 1.14 g (or 1 ml from the ink pipette) of ink added to it. This needs to be left for at least two minutes for the ink to distribute evenly on the rollers with the accelerated rollers in place. The ink should be used within half an hour of applying, as ink properties can change with temperature and loss of ink vehicle.

8.4 **SET UP THE IGT PRINT TESTER**

Follow the general guidelines given in the IGT Manual (see 4.3). The critical settings are:

- | | |
|---------------------|--|
| Rubber inking discs | - 5 cm (red rubber) |
| Sector packing | - None |
| Printing speed | - Constant; final speed 2.5 m/s (high range) |
| Printing force | - 625 N |
| Printing disc shaft | - Use the top shaft position |

NOTE 1: Use correction chart for setting the printing force. This chart is situated above the IGT Tester.

NOTE 2: The printing speed may be altered, depending on the testing requirements. Deviations from 2.0 m/s should be noted in test records.

8.5 PRINT TEST STRIPS USING CONSTANT LEVELS OF INK APPLICATION FOR EACH SET

The current scheme for test printing is to print four samples in parallel. Four replicates of each sample are printed in four sets. 0.15 ml of ink is added to each side of the inking unit with the IGT ink pipette in between each set of replicates. The ink is left for two minutes to re-distribute before the discs are inked up for the next set of replicates. Allow a minimum of 30 seconds for each disc to ink up. The discs are cleaned after printing each set.

8.6 CLEAN INK FROM PRINTING DISCS AND INKING ROLLERS

* Very soon after completing a series of prints, the ink should be removed from both the inking unit rollers and the printing discs. The best method is to use the rags provided and wipe off the majority of ink. Next, apply a minimum amount of blanket wash to remove the final amounts of ink.

NOTE: Gloves must be worn when using blanket wash, and the extraction fan in the fume cupboard must be on.

8.7 MEASURE THE SURFACE STRENGTH OF NEWSPRINT

* Leave the prints to dry for at least 15 minutes on the bench and then for at least 16 hours (preferably for two to three days) hanging in the CTH Room away from the light.

Follow the method in 140-A3-11-WI for measuring the surface strength of the newsprint samples using image analysis (the Optomax Speck Check).

Visually check the prints to ensure picking has actually taken place rather than “print misses”, which can occur on rough papers.

8.8 PREPARE REPORT

If a new or different sample of paper is used as a “standard” for comparative purposes, the new sample shall be compared with the old standard sample and the amount of picked fibre checked. The results will be filed in M Howards file and File No. 9.21.

- * It is important to report the detection level used to measure the pick strips (if it is not as detailed in 140-A3-11-WI) and the standard deviation or coefficient of variation, as this test is quite variable.

9.0 **SAFETY**

*

- Gloves must be worn when using blanket wash and the extraction fan in the fume cupboard must be running
- The fume cupboard fan should be left running for at least 10 minutes after cleaning
- All people using blanket wash should have a knowledge of the products health hazards and other safety information

This information is located next to the IGT printer

10.0 **ENVIRONMENTAL IMPACTS**

- * Used cleaning rags containing blanket wash should initially be disposed into a plastic bag inside the fume cupboard. This helps minimise any vapour inhalation.

Once the plastic bag is full, it should be sealed with sellotape and placed into the general rubbish paper bag.

APPENDIX B – National Print Laboratory, Procedure for IGT Testing

NPL Work Instruction

General Method for IGT Printability Tester AIC2-5

Purpose

To simulate offset and letterpress printing under controlled conditions in a laboratory. One or two colours can be printed. There are a large number of different tests that can be carried out using this equipment. This is a general procedure for operating the AIC2-5. For individual tests the appropriate IGT test method should be consulted.

Apparatus

1. IGT Printability Tester AIC2-5 Series 414.Z.
2. IGT High Speed Inking Unit 4.
3. Damson TLC2 thermostatic bath.
4. IGT ink pipette.
5. IGT printing disc(s).
6. Ink application chart.
7. Rags and cleaning solvent.

Safety Issues

1. When using volatile and/or flammable substances make sure the fume extraction system is switched on.
2. Do not wear any loose clothing, ties or jewellery that could get caught in the rotating rollers of the High Speed Inking Unit (HSIU) or any of the moving parts of the AIC2-5 tester. Long hair should be arranged so that it is not possible for it to become entangled in any of the moving parts of the AIC2-5 tester or the HSIU.
3. Make sure that the inks and solvents used do not come into contact with the skin or eyes. Wear protective clothing such as laboratory coats, gloves and safety glasses.
4. All used cleaning rags and other waste should be disposed of by placing in the red, automatically closing bins.
5. Any chemical waste should be stored in appropriate containers for later disposal. On no account should any chemical waste be poured down the sink.
6. Smoking and the use of naked flames are prohibited at any time in the laboratory.

Procedure

1. Before operating the TLC2 thermostatic bath check that the tank is filled to 1-2 cm below the lid. Add additional tap water if required.
2. Switch on the bath by turning the mains switch located on the front panel to the on position.
3. The bath is ready for use when a steady temperature of 22.5 degrees C is achieved.
4. Turn on the IGT High Speed Inking Unit (HSIU) with the switch at the bottom left-hand corner of the rear panel.
5. Place the appropriate rubber top roller (conventional or UV) into the holder on the inking unit.

6. Check that the distribution mode and disc ink-up times are set correctly. Refer to Sections 9.3-9.5 of the HSIU manual.
7. Place the printing disc(s) to be used on the shaft(s) of the HSIU. Allow the HSIU approximately 15 minutes to warm-up, with the rubber roller and printing disc(s) in contact.
8. Turn on the AIC2-5 printability tester by pressing the red coloured switch on the bottom left-hand side of the instrument.
9. Turn the operation switch to the on position – the pilot lamp immediately below the switch should light up.
10. Fit any required packing to the printing sector. If no packing is used, make sure to turn the large knurled screws clockwise as far as they will go to lock the packing clamps.
11. Cut the required number of test strips to the appropriate size. The maximum test strip size is 340 * 55 mm. Clamp the first sample to be tested onto the printing sector. The test strip may be clamped into either the front and rear clamps or the front clamp only.
12. Set the printing force for the printing disc(s) being used. Refer to Section 5.4 of the IGT AIC2-5 instruction manual.
13. Check the amount of free travel backlash in the printing disc lifters. If the amount of backlash is significantly greater than or less than 45 degrees of travel an adjustment will need to be made. The procedure for adjusting the amount of backlash is found in Section 5.5 of the instruction manual.
14. Set the printing speed as per the instructions in Section 5.6 of the AIC2-5 manual.
15. Bring the printing sector to the starting position. This is indicated by the pilot lamp on the top right-hand corner of the front panel lighting up.
16. Determine how much ink is required to obtain the desired ink film thickness by referring to IGT ink application chart.
17. Distribute the ink and ink-up the disc(s) as described in Section 10 of the instruction manual for the HSIU.
18. Place the inked printing disc(s) onto the appropriate spindles of the AIC2-5 tester. Push them on until they snap into position.
Note: The bottom spindle of the instrument cannot be used when testing in the accelerating speed mode.
19. Press the motor starter button with your right-hand and hold it in.
20. Turn the printing disc lifter(s) anticlockwise to the 'on' position.
21. When the motor has reached full speed press the sector starter button with your left-hand. Keep the motor and sector starter buttons pressed until the sector has completed the printing operation. When complete release both buttons.
22. Remove the test strip from the sector and place it aside for later assessment.
23. Turn the printing disc lifter(s) clockwise to the 'off' position and remove the printing disc(s) from the spindle(s) and set aside for cleaning.
24. The disk(s) need to be cleaned at the completion of each print. If this is not done the amount of ink applied to subsequent prints will not be as indicated on the IGT application chart. Cleaning should be completed by hand using a minimum amount of the appropriate solvent and a lint free rag.
25. The HSIU distribution rollers need to be cleaned at the completion of each set of four prints. Cleaning is carried out as per the instructions in Sections 9-10 of the HSIU manual.

26. At the completion of testing the following items need to be attended to:
- reset the printing force to zero on both printing stations
 - move the operation switch to the off position
 - turn off the power button on the bottom left-hand side of the AIC2-5 tester
 - turn off the HSIU and the thermostatic bath
 - thoroughly clean the printing discs, the HSIU distribution rollers and the ink pipette

APPENDIX C – Experimental Matrix for IGT Experiments

Sample	Ink Volume (ml)	Ink Thickness (μm)	Speed Mode	Speed (m/s)	Pressure	Ink Tank
1	0.35	8	constant	1		standard
2	0.35	8	Constant	1.25	800	standard
3	0.35	8	constant	1.5	800	standard
4	0.35	8	constant	2.0	800	standard
5	0.35	8	constant	3.0	800	standard
6	0.35	8	constant	4.0	800	standard
7	0.35	8	constant	5.0	800	standard
8	0.2	5	constant	1	800	standard
9	0.2	5	constant	2	800	standard
10	0.2	5	constant	3	800	standard
11	0.2	5	constant	4	800	standard
12	0.2	5	constant	5	800	standard
13	0.1	2.25	constant	1	800	standard
14	0.1	2.25	constant	2	800	standard
15	0.1	2.25	constant	3	800	standard
16	0.1	2.25	constant	4	800	standard
17	0.1	2.25	constant	5	800	standard
18	0.1	2.25	accelerating	7	800	standard
19	0.1	2.25	accelerating	5	800	standard
20	0.1	2.25	constant	5	800	high
21	0.35	8	constant	1	800	high
22	0.35	8	constant	1.5	800	high
23	0.35	8	constant	2.0	800	high
24	0.35	2.25	constant	3.0	800	high
25	0.35	2.25	constant	4.0	800	high
26	0.2	5	constant	4.0	800	standard
27	0.2	5	constant	4.0	800	standard
28	0.2	5	constant	5.0	800	standard
29	0.2	5	constant	5.0	800	standard
30	0.2	5	constant	4.5	800	standard
31	0.2	5	constant	4.5	800	standard
32	0.2	5	constant	4.0	800	standard
33	0.2	5	constant	4.0	800	standard
34	0.2	5	constant	4.0	800	standard
35	0.2	5	constant	4.0	800	standard
36	0.2	5	constant	4.0	800	standard
37	0.2	5	constant	2.5	800	standard
38	0.2	5	constant	2.5	800	standard
39	0.2	5	constant	2.5	800	standard
40	0.2	5	constant	2.5	800	standard

Sample	Ink Volume (ml)	Ink Thickness (μm)	Speed Mode	Speed (m/s)	Pressure	Ink Tank
41	0.2	5	constant	4	750	standard
42	0.2	5	constant	4	800	standard
43	0.2	5	constant	4	800	standard
44	0.2	5	constant	4	800	standard
45	0.2	5	constant	4	800	standard
46	0.2	5	constant	4	800	standard
47	0.2	5	constant	4	800	standard
48	0.2	5	constant	4	800	standard
49	0.2	5	constant	4	800	standard
20	0.2	5	constant	4	800	standard
51	0.2	5	constant	4	800	standard

APPENDIX D – Ink Weight on Printed IGT samples

Weight of Paper (g)	Weight of Paper + Ink (g)	Weight of Ink (g)
0.8604	0.8858	0.0254
0.8301	0.8536	0.0235
0.803	0.8278	0.0248
0.8674	0.8925	0.0251
0.8352	0.8607	0.0255
0.8636	0.8888	0.0252
0.8496	0.8749	0.0253
0.8565	0.8799	0.0234
0.8605	0.8832	0.0227
0.8704	0.8945	0.0241
0.8783	0.8997	0.0214
0.8185	0.8432	0.0247
0.8513	0.8739	0.0226
0.8455	0.8692	0.0237
0.8377	0.8607	0.023
0.8823	0.9058	0.0235
0.8843	0.908	0.0237
0.8334	0.858	0.0246
0.8451	0.8702	0.0251
0.8635	0.8883	0.0248
0.878	0.9015	0.0235
0.8544	0.8786	0.0242
0.874	0.8984	0.0244
0.8525	0.8774	0.0249
0.8844	0.9083	0.0239
0.8846	0.9111	0.0265

Average weight of ink on paper = 0.0242 g

Standard deviation = 0.0011 g

95 % Confidence Interval = 0.004 g

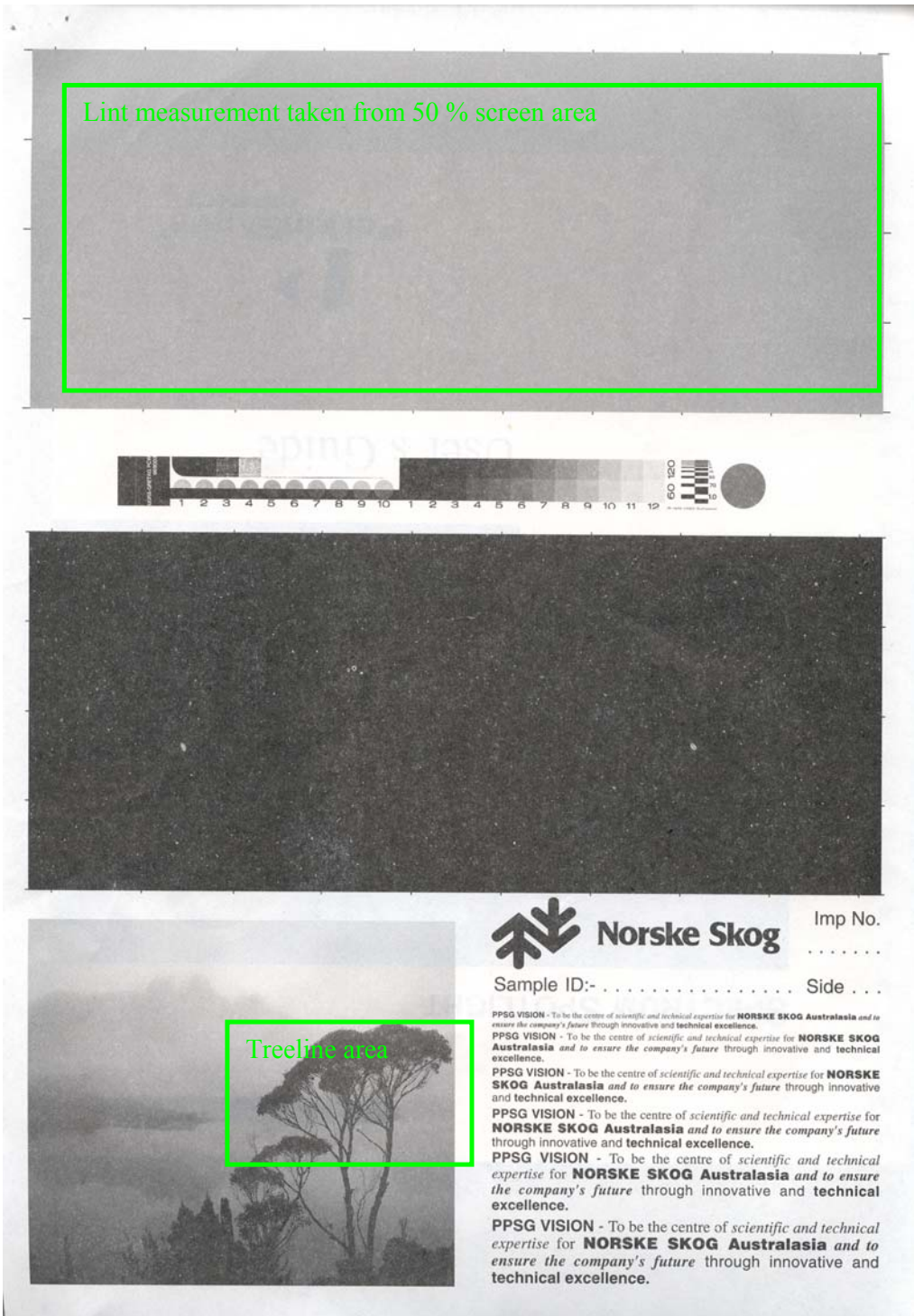
Area of Printed Image = 50mm x 208mm
= 0.0104 m²

Gsm of ink on printed image = $\frac{0.0242g}{0.0104m^2} = 2.33gm^{-2}$

APPENDIX E – Quantification of Printed IGT Lint

		0- 0.05	0.05 – 0.1	0.1 – 10	Total area	% 0 – 0.05	%0.05 – 0.1	% 0.1 - 10
Sample Identification		mm ²	mm ²	mm ²	mm ²			
B1	Top	47.97	10.39	16.13	74.50	64.40	13.95	21.66
B1	Bottom	65.61	12.75	16.04	94.40	69.50	13.51	16.99
B2	Top	31.21	6.88	7.11	45.20	69.05	15.22	15.73
B2	Bottom	73.09	14.20	18.35	105.65	69.18	13.45	17.37
B3	Top	68.17	9.52	9.98	87.67	77.75	10.86	11.38
B3	Bottom	112.89	30.64	47.18	190.70	59.20	16.07	24.74
B4	Top	24.85	3.82	2.98	31.65	78.52	12.06	9.42
B4	Bottom	91.46	13.85	9.14	114.45	79.92	12.10	7.99
B5	Top	22.12	2.17	2.01	26.30	84.10	8.25	7.65
B5	Bottom	61.66	9.66	4.97	76.29	80.82	12.67	6.52
B6	Top	63.41	8.73	8.74	80.88	78.40	10.79	10.81
B6	Bottom	106.73	20.81	18.86	146.40	72.90	14.21	12.88

APPENDIX F – Heidelberg Lint Test – Test Pattern



The image displays a Heidelberg Lint Test Test Pattern. At the top, a large rectangular area is outlined in green, with the text "Lint measurement taken from 50 % screen area" written inside in green. Below this is a color calibration strip featuring a grayscale ramp and various color patches, with numbers 1 through 12 and a circular target. The main body of the test pattern is a dark, textured rectangular area. At the bottom left, there is a photograph of a landscape with a treeline, where a specific area is outlined in green and labeled "Treeline area". To the right of the photograph is the Norske Skog logo, consisting of a stylized tree icon and the text "Norske Skog".

Imp No.

Sample ID:- Side ...

PPSG VISION - To be the centre of scientific and technical expertise for **NORSKE SKOG Australasia** and to ensure the company's future through innovative and technical excellence.

PPSG VISION - To be the centre of scientific and technical expertise for **NORSKE SKOG Australasia** and to ensure the company's future through innovative and technical excellence.

PPSG VISION - To be the centre of scientific and technical expertise for **NORSKE SKOG Australasia** and to ensure the company's future through innovative and technical excellence.

PPSG VISION - To be the centre of scientific and technical expertise for **NORSKE SKOG Australasia** and to ensure the company's future through innovative and technical excellence.

PPSG VISION - To be the centre of scientific and technical expertise for **NORSKE SKOG Australasia** and to ensure the company's future through innovative and technical excellence.

PPSG VISION - To be the centre of scientific and technical expertise for **NORSKE SKOG Australasia** and to ensure the company's future through innovative and technical excellence.

APPENDIX G– Particle Size Distribution of Filler in SEM backscatter images

Filler Area		Class 1	Class 2	Class 3	Class 4	Class 5	Total
Sample Identification		0 – 4 μm^2	4 - 8 μm^2	8–16 μm^2	16-50 μm^2	> 50 μm^2	μm^2
B1	Top	1727.13	472.76	376.80	377.24	109.93	3063.86
B1	Bottom	1784.69	454.80	357.31	349.89	109.72	3056.42
B2	Top	1810.31	393.17	289.53	253.94	97.93	2844.87
B2	Bottom	1504.22	336.55	203.87	170.60	26.54	2241.78
B3	Top	2361.09	601.04	491.51	603.25	356.70	4413.60
B3	Bottom	2465.82	723.62	617.08	714.90	689.86	5211.28
B4	Top	1596.28	362.27	230.01	180.60	33.72	2402.88
B4	Bottom	946.36	199.10	133.43	65.22	9.02	1353.12
B5	Top	2107.55	499.62	360.16	364.28	87.37	3418.97
B5	Bottom	1675.67	375.98	284.16	220.18	62.54	2618.53
B6	Top	1269.90	250.46	131.98	77.01	9.53	1738.88
B6	Bottom	740.61	151.16	93.43	59.11	11.83	1056.13

Number of particles		Class 1	Class 2	Class 3	Class 4	Class 5
Sample Identification		0 – 4 μm^2	4 - 8 μm^2	8–16 μm^2	16-50 μm^2	> 50 μm^2
B1	Top	1509.75	163.85	34.20	15.05	1.35
B1	Bottom	1581.25	166.65	33.15	13.85	1.60
B2	Top	1676.10	149.65	26.70	10.40	1.30
B2	Bottom	1358.85	145.55	19.00	7.05	0.40
B3	Top	2060.35	250.25	45.20	23.15	4.00
B3	Bottom	2118.85	219.15	56.30	27.95	6.90
B4	Top	1482.75	134.30	21.25	7.45	0.40
B4	Bottom	871.25	53.40	12.20	2.85	0.10
B5	Top	1905.40	177.75	33.45	15.50	1.25
B5	Bottom	1527.35	140.25	26.10	9.15	0.75
B6	Top	1159.80	122.85	12.30	3.25	0.15
B6	Bottom	677.70	47.90	8.65	2.60	0.15

These results are the averages of 20 individual images. The area for each image tested was 110 257.4 μm^2 .

% of Filler Area		Class 1	Class 2	Class 3	Class 4	Class 5
Sample Identification		0 – 4 μm^2	4 - 8 μm^2	8–16 μm^2	16-50 μm^2	> 50 μm^2
B1	Top	56.37	15.43	12.30	12.31	3.59
B1	Bottom	58.39	14.88	11.69	11.45	3.59
B2	Top	63.63	13.82	10.18	8.93	3.44
B2	Bottom	67.10	15.01	9.09	7.61	1.18
B3	Top	53.50	13.62	11.14	13.67	8.08
B3	Bottom	47.32	13.89	11.84	13.72	13.24
B4	Top	66.43	15.08	9.57	7.52	1.40
B4	Bottom	69.94	14.71	9.86	4.82	0.67
B5	Top	61.64	14.61	10.53	10.65	2.56
B5	Bottom	63.99	14.36	10.85	8.41	2.39
B6	Top	73.03	14.40	7.59	4.43	0.55
B6	Bottom	70.13	14.31	8.85	5.60	1.12

APPENDIX H – Specification sheet for Image / Norstar 52 gsm

APPENDIX I – Heidelberg Test results

Sample ID		Treeline Result	Heidelberg lint (gsm)
B0069368	B1-top		5.5
	B1-bottom	6	7.5
B0074346	B2-top		
	B2-bottom	8	7.2
B0067718	B3-top		
	B3-bottom	17	6.1
B0076485	B4-top		
	B4-bottom	3	6.8
B0076570	B5-top		
	B5-bottom	3	5.6
B0069624	B6-top		7.3
	B6-bottom	11	5.9